

Bragg resonance of waves in a two-layer fluid propagating over bottom ripples. Part I. Perturbation analysis

**MOHAMMAD-REZA ALAM,
YUMING LIU AND DICK K. P. YUE†**

Department of Mechanical Engineering, Center for Ocean Engineering,
Massachusetts Institute of Technology,
Cambridge, MA 02139, USA

(Received 29 November 2007 and in revised form 2 December 2008)

We investigate, via perturbation analyses, the mechanisms of nonlinear resonant interaction of surface-interfacial waves with a rippled bottom in a two-layer density-stratified fluid. As in a one-layer fluid, three classes of Bragg resonances are found to exist if nonlinear interactions up to the third order in the wave/ripple steepness are considered. As expected, the wave system associated with the resonances is more complicated than that in a one-layer fluid. Depending on the specifics of the resonance condition, the resonance-generated wave may be a surface or internal mode and may be transmitted or reflected. At the second order, class I Bragg resonance occurs involving two surface and/or internal waves and one bottom-ripple component. The interaction of an incident surface/internal wave with the bottom ripple generates a new surface or internal wave that may propagate in the same or the opposite direction as the incident wave. At the third order, class II and III Bragg resonances occur involving resonant interactions of four wave/ripple components: two surface and/or internal waves and two bottom-ripple components for class II resonance; three surface and/or internal waves and one bottom-ripple components for class III resonance. As in class I resonance, the resonance-generated wave in class II resonance has the same frequency as that of the incident wave. For class III resonance, the frequency of the resonant wave is equal to the sum or difference of the two incident wave frequencies. We enumerate and represent, using Feynman-like diagrams, the possible cases and combinations for Bragg resonance up to the third order (in two dimensions). Analytical regular perturbation results are obtained and discussed for all three classes of Bragg resonances. These are valid for limited bottom patch lengths and initial/finite growth of the resonant waves. For long bottom patches, a uniformly valid solution using multiple scales is derived for class I resonance. A number of applications underscoring the importance and implication of these nonlinear resonances on the evolution of ocean waves are presented and discussed. For example, it is shown that three internal/surface waves co-propagating over bottom topography are resonant under a broad range of Bragg conditions. The present study provides the theoretical basis and understanding for the companion paper (Alam, Liu & Yue 2008), where a direct numerical solution for the general nonlinear problem is pursued.

† Email address for correspondence: yue@mit.edu

1. Introduction

We consider the resonant interactions of waves in a two-layer density-stratified fluid travelling over bottom undulations. This work is motivated by the need for a better understanding of the mechanisms for the generation of internal waves, specifically in the littoral zone. While several generation mechanisms in this context have been proposed (Thorpe 1975; Garrett & Munk 1979; Miropol'sky 2001), the explanation for the presence of internal waves over continental shelves and lakes is still not resolved (Farmer & Armi 1999; Boegman *et al.* 2003; Cummins *et al.* 2003). The present work elucidates another possible mechanism for the generation of internal waves over rippled bottoms due to the resonant interaction among surface waves and bottom undulations. The nature of these classes of mechanisms require specific conditions, in terms of surface and bottom wavenumbers and layer depths, that may obtain under realizable situations, such as in large lakes (e.g. Antenucci & Imberger 2001) and over continental shelves (e.g. Holt & Thorpe 1997).

The problem we consider is similar to, and is an extension of, the case of a homogeneous fluid, in that waves are modified as they travel over and interact with non-uniform bottom topography. Unlike the case of a homogeneous fluid, however, in a two-layer fluid, there are two free-wave solutions at a given frequency: a surface-mode and an internal-mode solution. Of great interest is when they – along with the bottom topography – satisfy the so-called Bragg condition in which the rate of energy exchange is maximum. When an incident wave hitting the rippled region satisfies this condition the resonant wave can then be a reflected/transmitted surface-/internal-mode wave. Bragg resonance in stratified fluids, besides offering a new mechanism for the generation of internal waves, affects the development of the wave spectrum in the coastal regions and continental shelves (e.g. Ball 1964) and modifies the shore-parallel sandbars (e.g. Heathershaw & Davies 1985).

In the simpler case of a homogeneous fluid, the interaction of surface waves with bottom undulations has been studied extensively, owing to its importance in the formation of near-shore sandbars and the evolution of ocean wave field in littoral zones. Davies (1982) used regular perturbation analysis to find the amplitude growth rate of the resonant wave at and near the resonance. His solution becomes unbounded when the number of bottom ripples increases indefinitely. To overcome this, Mei (1985) invoked a multiple-scale analysis to derive a uniformly convergent solution for the interacting wave components. Kirby (1986) gave a similar solution by extending the mild-slope equation to include the effect of fast bottom undulations. By including higher order interactions, Liu & Yue (1998) generalized the second-order Bragg resonance to include third-order quartet resonant interactions of waves and bottom ripples.

In the absence of bottom non-uniformity, the dynamics of internal wave propagation and interaction is relatively well understood (see for example Gargett & Hughes 1972; Olbers & Herterich 1979; Kudryavtsev 1994), although their generation mechanisms are still a subject of active research (see, e.g., Farmer & Armi 1999). The nonlinear resonant interactions between surface and interfacial waves was studied by Ball (1964) who considered a resonant triad formed by two surface-mode wave components and one internal-mode wave component. Later, Wen (1995) (also see Hill & Foda 1996, 1998; Jamali 1998; Jamali, Lawrence & Seymour 2003; Hill 2004) showed that resonance may occur between two internal-mode waves and one surface-mode wave.

In the presence of the bottom topography and invoking a rigid-lid assumption, Baines (1997) studied the interaction of internal waves with bottom non-uniformities.

McKee (1996) extended the modified mild-slope equation of Kirby (1986) to a two-layer fluid and investigated the second-order resonant interaction among a surface incident wave, an internal wave and a sinusoidal bottom undulation. Over a random bathymetry Alam & Mei (2007) and Chen & Liu (1996) studied the localization of internal waves under the rigid-lid assumption.

The objective of this work is to consider the general nonlinear resonance interactions involving surface and internal waves in two-layer density-stratified fluid travelling over a wavy bottom. Of special interest are the higher order (generalized) Bragg resonances that may play an important role especially in near-shore and estuary areas, where stratification layers are relatively shallow and comparable in depth.

We provide in §2 an analysis of the conditions for generalized Bragg resonances for nonlinear interactions of surface/internal waves with bottom ripples up to the third order in the wave/ripple steepness. At the second order, class I Bragg resonance condition obtains wherein a resonant triad can be formed with an incident wave, a bottom-ripple component and a resonance-generated wave. The resonance-generated wave has the same frequency as the incident wave. Depending on the wave numbers of the incident wave and bottom ripples, the generated wave can be a surface- or an internal-mode wave travelling in the same or the opposite direction as the incident wave. We enumerate the various triad combinations and categorize them schematically in Feynman-diagram-like representations. For steep waves and bottom ripples, (generalized) Bragg resonances at the third order may be important, involving quartet interactions among free-surface/internal and bottom modes. Specifically, two types of resonant quartets can be formed. One involves two free-wave components (surface or internal mode) and two bottom-ripple components, and the other involves three propagating-wave components (surface or internal mode) and one bottom component. For convenience in description and following existing convention for one-layer fluid (see Liu & Yue 1998), the former and latter are respectively called class II and class III Bragg resonances. Class II resonance is similar to class I in characteristic, except there are now two bottom-ripple components participating in the resonance. In class III Bragg resonance, for the resonant quartet, two of the three propagating-wave components can in general be considered incident waves, and the third one is then regarded the resonance-generated wave. Unlike class I and class II resonances, the frequency of this generated wave equals the sum or difference of the frequencies of the two incident waves. As in class I and class II resonances, the generated wave may be reflected or transmitted and may be surface- or internal-mode depending on the wavenumber combination of the incident waves and bottom ripples. For class III Bragg resonance, a total of 48 different cases are enumerated.

To understand the mechanisms and characteristics of the resonances, we perform perturbation analyses of these cases. In §3, we use a regular perturbation technique to obtain the (initial) growth near the resonance for all three classes of Bragg resonance. As the number of ripples (or interaction distance) increases indefinitely, regular perturbation becomes invalid and fails to predict strong Bragg reflection/transmission. To overcome this difficulty, a multiple-scale analysis is utilized in §4 to study strong reflection/transmission for class I Bragg resonance. Multiple-scale analyses can in principle also be obtained for higher order resonances (see e.g. Hill 2004, for a special case of deep layers without bottom undulations), but the algebra is proportionately more involved and is not pursued here. For the general problem with increasing number of resonant mechanisms at high orders, a full theoretical treatment is, in any event, impractical, and a direct numerical approach is needed (see Alam *et al.* 2008). Finally, in §5, we discuss a number of cases in which the interactions we study have

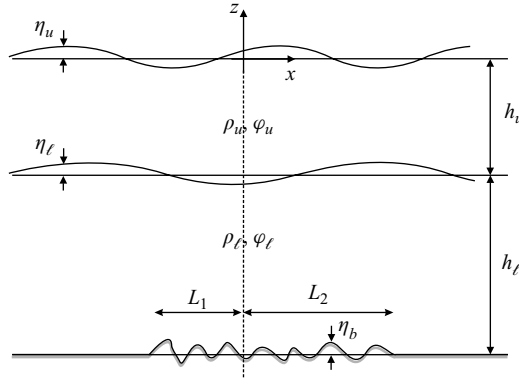


FIGURE 1. Definition sketch of waves on a two-layer fluid over a rippled bottom.

appreciable effect on resonant internal-/surface-wave generation or introduce new mechanisms for such generation.

In realistic situations, the surface-/internal-mode waves and bottom undulations in general may contain many components. Depending on the steepness and the size of the interacting domain, multiple resonances at different orders may obtain. The analytic results in this paper provide a basis for understanding these nonlinear interactions. For useful quantitative predictions of the surface-/internal-wave environment, one needs to resort to effective direct numerical simulations. This is the subject of the companion paper (Alam *et al.* 2008).

2. Resonance condition

2.1. Statement of the problem

We consider a two-layer fluid with incident wave(s) propagating over non-uniform bottom topography, subject to the condition of relatively mild surface-/interface-/bottom-wave slopes. Of basic interests here are the conditions involving the incident wave and bottom topography wavenumbers for given fluid-layer depths and density ratios for which (generalized) Bragg resonant interactions obtain.

2.1.1. Governing equations

We define a Cartesian coordinate system with x -axis on the mean free surface and z -axis positive upward. We consider a two-layer density-stratified fluid, where the upper and lower fluid layers have respectively mean depths h_u and h_ℓ and fluid densities ρ_u and ρ_ℓ (with the subscripts u and ℓ hereafter denoting quantities associated with the upper and lower fluid layers, respectively). The two-layer fluid rests on a rippled horizontal bottom given by $z = -h_u - h_\ell + \eta_b$, where η_b is the elevation of the bottom undulation measured from mean bottom depth (see figure 1).

We assume that the fluids in both layers are homogeneous, incompressible, immiscible and inviscid so that the fluid motion is irrotational. The effect of surface tension is neglected. The flow in each layer is described by a velocity potential, $\phi_u(x, z, t)$ and $\phi_\ell(x, z, t)$. The exact nonlinear equations (applied on/within actual boundary positions) governing the potential flow in the two-layer fluid are

$$\nabla^2 \phi_u = 0, \quad -h_u + \eta_\ell < z < \eta_u, \quad (2.1a)$$

$$\nabla^2 \phi_\ell = 0, \quad -h_u - h_\ell + \eta_b < z < -h_u + \eta_\ell, \quad (2.1b)$$

$$\begin{aligned} \phi_{u,tt} + g\phi_{u,z} + (\partial_t + 1/2 \phi_{u,x}\partial_x \\ + 1/2 \phi_{u,z}\partial_z)(\nabla\phi_u \cdot \nabla\phi_u) = 0, \quad z = \eta_u, \end{aligned} \quad (2.1c)$$

$$g\eta_u + \phi_{u,t} + 1/2 (\nabla\phi_u \cdot \nabla\phi_u) = 0, \quad z = \eta_u, \quad (2.1d)$$

$$\begin{aligned} \mathcal{R}\{\phi_{u,tt} + g\phi_{u,z} + 1/2 (\nabla\phi_u \cdot \nabla\phi_u)_{,t} + \eta_{\ell,t}[\phi_{u,t} \\ + 1/2 (\nabla\phi_u \cdot \nabla\phi_u)_{,z} - g\eta_{\ell,x}\phi_{u,x}\} - \{\phi_{\ell,tt} \\ + g\phi_{\ell,z} + 1/2 (\nabla\phi_\ell \cdot \nabla\phi_\ell)_{,t} + \eta_{\ell,t}[\phi_{\ell,t} \\ + 1/2 (\nabla\phi_\ell \cdot \nabla\phi_\ell)_{,z} - g\eta_{\ell,x}\phi_{\ell,x}\} = 0, \quad z = -h_u + \eta_\ell, \end{aligned} \quad (2.1e)$$

$$\eta_{\ell,t} + \eta_{\ell,x}\phi_{u,x} - \phi_{u,z} = 0, \quad z = -h_u + \eta_\ell, \quad (2.1f)$$

$$\eta_{\ell,t} + \eta_{\ell,x}\phi_{\ell,x} - \phi_{\ell,z} = 0, \quad z = -h_u + \eta_\ell, \quad (2.1g)$$

$$\eta_{b,x}\phi_{\ell,x} - \phi_{\ell,z} = 0, \quad z = -h_u - h_\ell + \eta_b, \quad (2.1h)$$

where $\mathcal{R} \equiv \rho_u/\rho_\ell$ is the density ratio; $\eta_u(x, t)$ and $\eta_\ell(x, t)$ are the elevations of the free-surface and the interface respectively; and g is the gravity acceleration.

2.1.2. Regular perturbation expansion

For small surface η_u and interfacial η_ℓ waves over a mildly varying bottom topography η_b , we expand the velocity potentials (ϕ_u and ϕ_ℓ) and the wave elevations (η_u and η_ℓ) in perturbation series with respect to a small parameter ϵ that measures the wave/bottom steepnesses which are assumed, for simplicity, to be of the same order:

$$\phi_u = \epsilon\phi_u^{(1)} + \epsilon^2\phi_u^{(2)} + O(\epsilon^3), \quad \phi_\ell = \epsilon\phi_\ell^{(1)} + \epsilon^2\phi_\ell^{(2)} + O(\epsilon^3), \quad (2.2a)$$

$$\eta_u = \epsilon\eta_u^{(1)} + \epsilon^2\eta_u^{(2)} + O(\epsilon^3), \quad \eta_\ell = \epsilon\eta_\ell^{(1)} + \epsilon^2\eta_\ell^{(2)} + O(\epsilon^3). \quad (2.2b)$$

Substituting (2.2) into (2.1), expanding the quantities on the free surface, interface and bottom in Taylor series with respect to the respective mean positions and collecting terms at each order $m = 1, 2, \dots$, we obtain

$$\nabla^2\phi_u^{(m)} = 0, \quad -h_u < z < 0, \quad (2.3a)$$

$$\nabla^2\phi_\ell^{(m)} = 0, \quad -h_u - h_\ell < z < -h_u, \quad (2.3b)$$

$$\phi_{u,tt}^{(m)} + g\phi_{u,z}^{(m)} = f_1^{(m)}, \quad z = 0, \quad (2.3c)$$

$$g\eta_u^{(m)} + \phi_{u,t}^{(m)} = f_2^{(m)}, \quad z = 0, \quad (2.3d)$$

$$\mathcal{R}(\phi_{u,tt}^{(m)} + g\phi_{u,z}^{(m)}) - (\phi_{\ell,tt}^{(m)} + g\phi_{\ell,z}^{(m)}) = f_3^{(m)}, \quad z = -h_u, \quad (2.3e)$$

$$\phi_{u,z}^{(m)} - \phi_{\ell,z}^{(m)} = f_4^{(m)}, \quad z = -h_u, \quad (2.3f)$$

$$\eta_{\ell,t}^{(m)} - \phi_{u,z}^{(m)} = f_5^{(m)}, \quad z = -h_u \quad (2.3g)$$

$$\phi_{\ell,z}^{(m)} = f_6^{(m)}, \quad z = -(h_u + h_\ell), \quad (2.3h)$$

where $f_j^{(1)} = 0$ for $j = 1, \dots, 6$ and $f_j^{(m)}$ for $m \geq 2$, $j = 1, \dots, 6$ are functions of lower order quantities. In a regular perturbation, the linear equation system (2.3) are solved successively to higher order starting from $m = 1$.

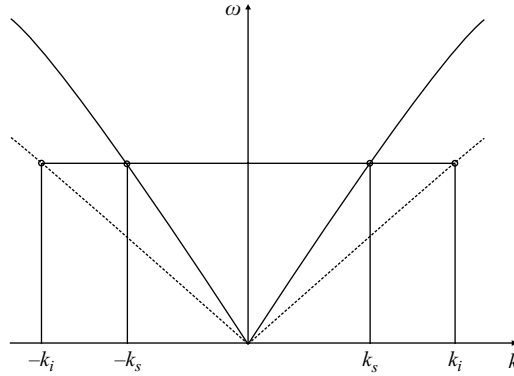


FIGURE 2. Sketch of the dispersion relation for wavenumber k and frequency ω of a free wave in a two-layer fluid. Dashed lines correspond to the internal mode, and the solid lines correspond to the surface mode.

2.1.3. Linear solution

At $m = 1$, (2.3) is homogeneous, and the eigensolution representing a free propagating wave can be written as (see Lamb 1932)

$$\eta_u^{(1)} = a \cos(kx - \omega t), \tag{2.4a}$$

$$\eta_\ell^{(1)} = b \cos(kx - \omega t), \tag{2.4b}$$

$$\phi_u^{(1)} = (A \cosh kz + B \sinh kz) \sin(kx - \omega t), \tag{2.4c}$$

$$\phi_\ell^{(1)} = C \cosh k(z + h_u + h_\ell) \sin(kx - \omega t), \tag{2.4d}$$

where ω and k represent the frequency and wavenumber of the wave, respectively. The coefficients a and b are the amplitudes of waves on the surface and the interface and are related by

$$\frac{b}{a} = \cosh kh_u - \frac{gk}{\omega^2} \sinh kh_u. \tag{2.5}$$

In terms of a and b , the coefficients A , B and C are given by

$$A = \frac{ga}{\omega}, \quad B = \frac{\omega a}{k}, \quad C = \frac{\omega b}{k \sinh kh_\ell}. \tag{2.6}$$

In (2.4), ω and k satisfy the dispersion relation

$$\mathcal{D}(k, \omega) \equiv \omega^4(\mathcal{R} + \coth kh_u \coth kh_\ell) - \omega^2 gk(\coth kh_u + \coth kh_\ell) + g^2 k^2(1 - \mathcal{R}) = 0. \tag{2.7}$$

For a given ω , (2.7) possesses two pairs of real roots for the wavenumber k (Ball 1964). The variation of these roots as a function of the frequency is sketched in figure 2, which we hereafter refer to as Ball’s diagram. In figure 2, the steeper (milder) sloped pair of branches with smaller (greater) $|k|$ for given ω is referred to as the surface (internal) mode. A surface-mode (or an internal-mode) wave is a freely propagating wave that has a surface elevation *and* an interface elevation. Therefore we may talk, for example, about the interface elevation of a surface-mode wave, i.e. (2.4b), when ω, k are associated with a surface-mode wave which is the inner branch of the Ball’s diagram. The qualitative difference between the surface and internal modes can be seen more readily by considering the case of weak stratification (\mathcal{R} close to 1): the

sign of b/a in (2.5) is positive (negative) for the surface (internal) mode, and therefore the phases of the surface elevation $\eta_u^{(1)}$ and the interfacial elevation $\eta_\ell^{(1)}$ are the same (π radian different); also the free surface-wave amplitude a is greater (smaller) than that of the lower surface (interface) amplitude b . As the density ratio \mathcal{R} varies from 0 to 1, the surface-mode branch does not change much, while the internal-mode branch moves from the vicinity of the surface-mode branch (as $\mathcal{R} \rightarrow 0$) towards the wavenumber axis (as $\mathcal{R} \rightarrow 1$).

2.2. Class I Bragg resonance

Consider a right-going incident wave of frequency ω and wavenumber k , propagating over a rippled bottom with the elevation given by

$$\eta_b(x) = d \sin(k_b x), \quad (2.8)$$

where d and k_b are respectively the amplitude and wavenumber of the bottom undulations. The incident wave can be either surface mode or internal mode given by (2.4).

At the second order ($m=2$), the inhomogeneous terms $f_j^{(2)}$, $j=1, \dots, 6$, take the form

$$f_1^{(2)} = -\eta_u^{(1)} \phi_{u,zz}^{(1)} - g \eta_u^{(1)} \phi_{u,zz}^{(1)} - (\nabla \phi_u^{(1)} \cdot \nabla \phi_u^{(1)})_t, \quad (2.9a)$$

$$f_2^{(2)} = -\eta_u^{(1)} \phi_{u,zt}^{(1)} - \frac{1}{2} (\nabla \phi_u^{(1)} \cdot \nabla \phi_u^{(1)}), \quad (2.9b)$$

$$f_3^{(2)} = [(\eta_\ell^{(1)} \phi_{\ell,z}^{(1)})_t - g (\eta_\ell^{(1)} \phi_{\ell,x}^{(1)})_x + \frac{1}{2} (\nabla \phi_\ell^{(1)} \cdot \nabla \phi_\ell^{(1)})_t], z \\ - \mathcal{R} [(\eta_\ell^{(1)} \phi_{u,zt}^{(1)})_t - g (\eta_\ell^{(1)} \phi_{u,x}^{(1)})_x + \frac{1}{2} (\nabla \phi_u^{(1)} \cdot \nabla \phi_u^{(1)})_t], \quad (2.9c)$$

$$f_4^{(2)} = [\eta_\ell^{(1)} (\phi_u^{(1)} - \phi_\ell^{(1)})_x]_x, \quad (2.9d)$$

$$f_5^{(2)} = -(\eta_\ell^{(1)} \phi_{u,x}^{(1)})_x, \quad (2.9e)$$

$$f_6^{(2)} = (\eta_b \phi_{\ell,x}^{(1)})_x. \quad (2.9f)$$

Substituting (2.4) and (2.8) into (2.9) shows that $f_6^{(2)}$ contains a term with a factor of $\sin[(k \pm k_b)x - \omega t]$, which is associated with the interaction of a surface-/internal-mode wave and bottom ripples. If $k \pm k_b$ and ω satisfy the dispersion relation, i.e.

$$\left. \begin{aligned} \mathcal{D}(k_r, \omega) &= 0, \\ k_r &= k \pm k_b, \end{aligned} \right\} \quad (2.10)$$

where the subscript r denotes the resonant wave; the interaction term is secular; and the second-order interaction becomes resonant. As a result, a free propagating wave of wavenumber k_r and frequency ω is generated. The surface (η_u) and interfacial (η_ℓ) elevations of this wave are determined from (2.3) (with $m=2$) to be

$$\eta_u^{(2)}, \eta_\ell^{(2)} \propto t \sin(k_r x - \omega t) \quad (2.11)$$

for a long uniformly rippled bottom. Under this condition, (2.11) shows that the amplitude of the generated wave grows indefinitely over time.

As in a one-layer fluid (e.g. Liu & Yue 1998), we call (2.10) the class I Bragg condition. For a given incident wave (or bottom ripple) wavenumber, the requisite wavenumber of bottom ripples (or incident wave) for class I resonance can be derived directly from figure 2. For convenience, we denote the wavenumber of the incident

wave generally as k and write k as k_s (k_i) if it is a surface- or internal-mode wave. For $k = k_s$, class I resonance happens if $k_b = k_i - k_s$, $k_b = 2k_s$ or $k_b = k_s + k_i$. On the other hand, for $k = k_i$, class I resonance obtains if $k_b = k_i - k_s$, $k_b = 2k_i$ or $k_b = k_s + k_i$.

Interaction of waves with bottom topography in some aspects resembles the interaction of particles in quantum electrodynamics (QED), where Feynman diagrams are commonly used to schematically represent the different interaction processes. In the present context, we find the use of Feynman-like diagrams to represent the resonant interactions even more intuitive. (For another use of such diagrams in a related context, see Hasselmann 1966.)

The left-hand side of figure 3 shows the use of this schematic representation to illustrate all six cases of class I Bragg resonance. In each diagram, a surface-mode, an internal-mode and an undulatory-bottom component is depicted respectively by a solid, a dashed and a wavy line. The directions of each of the incident, reflected and transmitted waves are indicated by arrows. In all diagrams we assume that the incident wave always comes from the far left. Since only one frequency (i.e. ω) participates in class I Bragg resonance the resonance condition can be written solely in terms of wavenumbers. This condition is given immediately below each corresponding diagram in figure 3. The interpretation of these diagrams is direct and straightforward. For example, in the left (class I) column, the second diagram represents a class I Bragg resonance between an incident surface-mode wave and the wavy bottom. If the wavenumber of the wavy bottom satisfies $k_b = k_s + k_i$, where each of k_i and k_s and the frequency ω satisfy the dispersion relation, then the resonant wave will be a reflected (i.e. left-going) internal-mode wave with the wavenumber k_i . Part of the incident wave with the wavenumber k_s continues to travel to the right without change as indicated by the solid arrow (labelled k_s) going to the right.

These six cases can be classified into three groups based on whether the energy exchange happens between two different modes (i.e. a surface-mode wave gives its energy to an internal-mode wave or vice versa) or between similar modes and if the resonant wave is a transmitted or a reflected wave. Based on this, the six cases of class I Bragg resonance we found can be grouped into the following: (i) inter-modes in transmission, $S_c \xrightarrow{k_b} I_T$ and $I_c \xrightarrow{k_b} S_T$; (ii) inter-modes in reflection, $S_c \xrightarrow{k_b} I_R$ and $I_c \xrightarrow{k_b} S_R$; and (iii) same-mode in reflection, $S_c \xrightarrow{k_b} S_R$ and $I_c \xrightarrow{k_b} I_R$. In these, S and I stand for surface-mode and internal-mode respectively, and subscripts c , R and T denote incident, reflected and transmitted waves respectively. For (i)/(ii), energy exchange occurs between surface mode and internal mode of waves that travel in the same/opposite direction. For (iii), energy exchange occurs in the same mode of waves travelling in the opposite direction. Case (iii) is the direct extension of the result in a one-layer fluid (see Liu & Yue 1998) to a two-layer fluid.

The number of cases in figure 3 is reduced in conditions of ocean stratification, where $1 - \mathcal{R} \ll 1$. In particular, two of these involving incident internal-mode waves and resonant surface-mode waves, i.e. $I_c \xrightarrow{k_b} S_T$ and $I_c \xrightarrow{k_b} S_R$, give vanishing growth rates, while their counterparts, $S_c \xrightarrow{k_b} I_T$ and $S_c \xrightarrow{k_b} I_R$, may lead to finite growth rates and are shown to offer a potential mechanism for the generation of high-frequency internal waves (§ 5.3). For $\mathcal{R} \rightarrow 1$, the case $S_c \xrightarrow{k_b} S_R$ reduces to the homogeneous-fluid Bragg resonance, and the case $I_c \xrightarrow{k_b} I_R$ is effectively one involving a two-layer fluid under a rigid surface, in which case the analysis can be much simplified (see for example Baines 1995, for a discussion on the validity of the rigid lid assumption). As

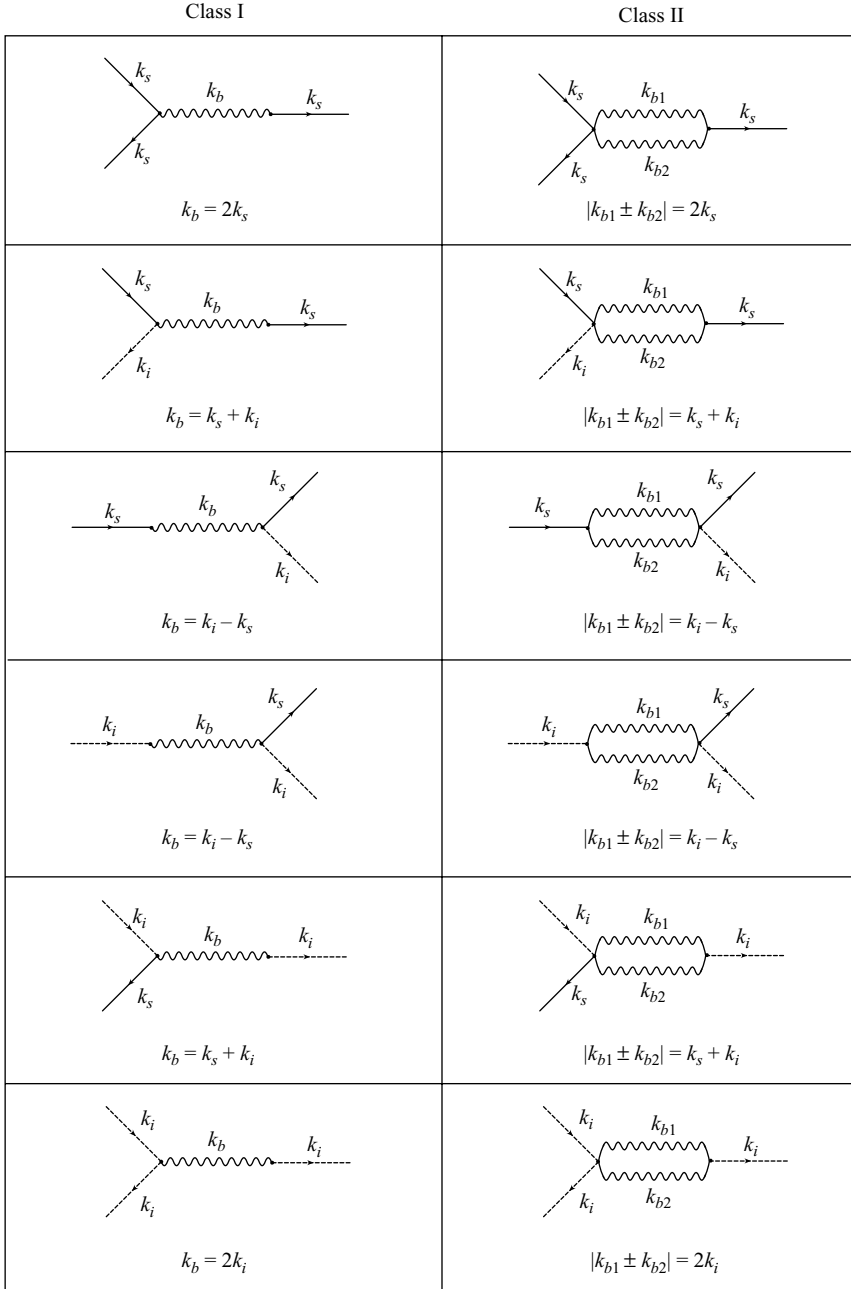


FIGURE 3. Feynman diagram representations of class I (left) and II (right) Bragg resonance conditions in a two-layer fluid. The solid, dashed and wavy lines respectively represent surface-, internal- and bottom-wave components. Arrows indicate the direction of wave propagation.

is shown later, $I_c \xrightarrow{k_b} I_R$ leads to non-vanishing growth rates in the limit $1 - \mathcal{R} \ll 1$ (see figure 5) and can be responsible for partial reflection of internal waves over continental shelves (§ 5.2).

2.3. Class II Bragg resonance

As expected, resonance interactions occur also at the third order ($m = 3$), involving quartets of propagating/bottom modes. These belong to two broad types: one consists of two free-wave and two bottom-ripple components and the other of three wave components and one bottom component. As in the case of Bragg scattering in a one-layer fluid (Liu & Yue 1998), the resonance associated with the former/latter quartet wave–bottom interaction is denoted as class II/III Bragg resonance.

To illustrate the class II Bragg resonance condition, we consider a bottom elevation is given by the superposition of two ripple components of wavenumbers k_{b1} and k_{b2} . Upon carrying out the perturbation analysis to the third order (with (2.4) as the first-order solution), we obtain that the bottom forcing $f_6^{(3)}$ in (2.3) contains terms proportional to $\sin[(k \pm 2k_{b1})x - \omega t]$, $\sin[(k \pm 2k_{b2})x - \omega t]$ and $\sin[(k \pm k_{b1} \pm k_{b2})x - \omega t]$. Class II Bragg resonance occurs whenever the wavenumber $k \pm 2k_{b1}$ or $k \pm 2k_{b2}$ or $k \pm k_{b1} \pm k_{b2}$ and the frequency ω satisfy the dispersion relation (2.7). Thus, in general form, the class II Bragg resonance condition can be expressed as

$$\left. \begin{aligned} \mathcal{D}(k_r, \omega) &= 0, \\ k_r &= k \pm k_{b1} \pm k_{b2} \end{aligned} \right\} \quad (2.12)$$

The class II resonance condition (2.12) is identical to the class I resonance condition (2.10) if k_b in (2.10) is replaced by the super- or sub-harmonic combination of the two bottom-ripple components $k_{b1} \pm k_{b2}$. Class II resonance is thus a direct extension of class I resonance to the third order. Like class I, there are also six cases of class II resonance, which are schematically illustrated in the right column of figure 3. For realistic ocean stratifications, these cases reduce similarly to that in Class I, and the discussion at the end of §2.2 applies here as well. Finally, we note that class II resonance may also obtain when the bottom contains only one ripple component, given from (2.12) by setting $k_{b1} = k_{b2}$.

2.4. Class III Bragg resonance

In class III Bragg resonance, the resonant quartet is composed of three travelling waves and one bottom-ripple component. To obtain this resonance condition, we consider the general case involving two incident waves of wavenumbers k_1 and k_2 and frequencies ω_1 and ω_2 . Without loss of generality, we assume $k_1 > |k_2| > 0$. Starting with the linear solution for the two free-wave components and carrying out the perturbation analysis in (2.3) to the third order, we obtain that the inhomogeneous terms, $f_j^{(3)}$, $j = 1, \dots, 6$, contain terms proportional to $\sin[(2k_1 \pm k_b)x - 2\omega_1 t]$, $\sin[(2k_2 \pm k_b)x - 2\omega_2 t]$ and $\sin[(k_1 \pm k_2 \pm k_b)x - (\omega_1 \pm \omega_2)t]$. If the combined wavenumber and frequency in any of these forcing terms satisfy the dispersion relation, the associated wave–bottom interaction becomes resonant, and a third free-wave component is generated by the resonance. The condition for class III Bragg resonance can be written in the following general form:

$$\left. \begin{aligned} \mathcal{D}(k_r, \omega_r) &= 0, \\ k_r &= k_1 \pm k_2 \pm k_b, \quad \omega_r = \omega_1 \pm \omega_2 \end{aligned} \right\} \quad (2.13)$$

in which k_r and ω_r represent the wavenumber and frequency of the resonant generated wave.

Due to the involvement of three free propagating waves, combinations of wave components in class III resonance are more complicated than those in class II resonance. Figure 4 shows schematic representations of all possible wave–ripple combinations satisfying the class III resonance condition (2.13). In figure 4, the

Class III

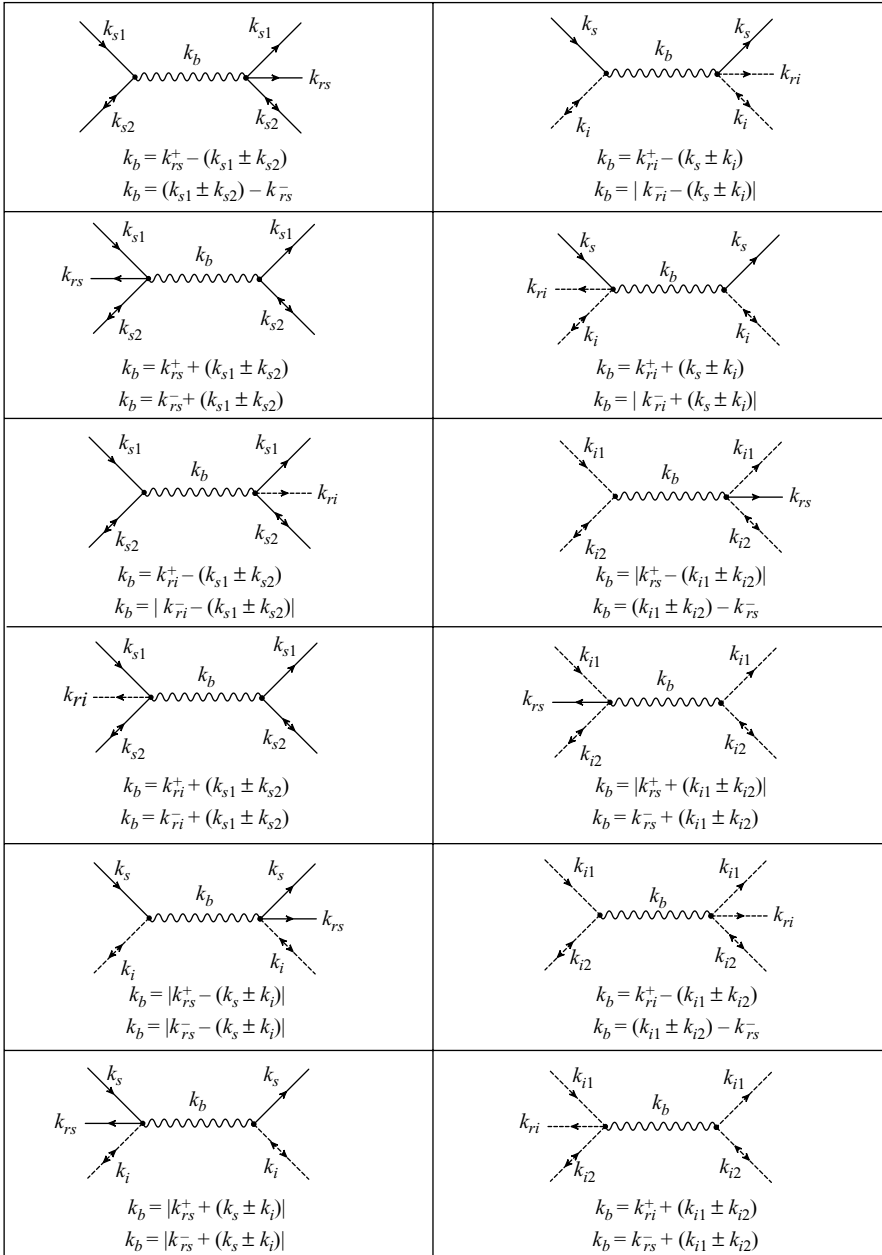


FIGURE 4. Feynman diagram representations of class III Bragg resonance conditions in a two-layer fluid. The solid, dashed and wavy lines respectively represent surface-, internal- and bottom-wave components. Arrows indicate the direction of wave propagation. Each diagram shows four cases. The line with double-sided arrow shows two cases when a right-going wave gives another right-going wave on the other side of the ripples and when a left-going wave gives another left-going wave on the other side of the ripples.

resonant wave is indicated by the subscript ‘ r ’, which has frequency of either $\omega_1 + \omega_2$ (corresponding to superscript $+$) or $\omega_1 - \omega_2$ (corresponding to superscript $-$), and it can be either a surface-mode wave or an internal-mode wave indicated respectively by an additional subscript s or i .

As an illustration, consider the first case of figure 4. This case represents four possible interactions between two surface-mode waves (k_{s1}, k_{s2}) that result in a transmitted surface-mode wave (k_{rs}). The resonant generated surface-mode wave with wavenumber k_{rs} can have two possible frequencies: (1) $\omega_1 + \omega_2$, therefore denoted by k_{rs}^+ , i.e. $\mathcal{D}(k_{rs}^+, \omega_1 + \omega_2) = 0$; (2) $\omega_1 - \omega_2$, hence denoted by k_{rs}^- with $\mathcal{D}(k_{rs}^-, \omega_1 - \omega_2) = 0$. If two incident waves travel in the same direction (from the left to the right), then only right arrows have to be picked up for the correct representation. In this case, there are two bottom wavenumbers that can cause the incident wave to resonate a new wave: if $k_b = k_{rs}^+ - (k_{s1} + k_{s2})$ or $k_b = k_{s1} - k_{s2} - k_{rs}^-$. If two incident waves travel in opposite directions, we assume k_{s1} moves rightward and k_{s2} moves leftward; hence left arrows on k_{s2} lines must be chosen. In this case a transmitted surface-mode wave can be generated if $k_b = k_{rs}^+ - (k_{s1} - k_{s2})$ or $k_b = k_{s1} + k_{s2} - k_{rs}^-$. Note that although the resonant wave can have a positive or negative wavenumber in (2.13), for clarity in the diagrams in figure 4, wavenumbers are always given as positive, and the wave direction is indicated by the arrow.

As before, the resonance cases in figure 4 can be classified in terms of the energy exchange among surface-/internal-wave modes and propagation direction of the resonance-generated wave. There are four such categories: (i) inter-modes in transmission $S_{c1} + S_{c2} \xrightarrow{k_b} I_T$, $I_c + S_c \xrightarrow{k_b} S_T$, $I_c + S_c \xrightarrow{k_b} I_T$ and $I_{c1} + I_{c2} \xrightarrow{k_b} S_T$; (ii) inter-modes in reflection, $S_{c1} + S_{c2} \xrightarrow{k_b} I_R$, $I_c + S_c \xrightarrow{k_b} S_R$, $I_c + S_c \xrightarrow{k_b} I_R$ and $I_{c1} + I_{c2} \xrightarrow{k_b} S_R$; (iii) same-mode in reflection, $S_{c1} + S_{c2} \xrightarrow{k_b} S_R$ and $I_{c1} + I_{c2} \xrightarrow{k_b} I_R$; and (iv) same-mode in transmission, $S_{c1} + S_{c2} \xrightarrow{k_b} S_T$ and $I_{c1} + I_{c2} \xrightarrow{k_b} I_T$. One notes that in the above, (i) and (ii) are unique for a two-layer fluid, while (iii) and (iv) are a direct extension of class III resonances in a one-layer fluid (Liu & Yue 1998).

As in figure 3, not all the cases in figure 4 are important in conditions of weak ocean stratification. For instance, the growth rate for the case $I_{c1} + I_{c2} \xrightarrow{k_b} S_R$ vanishes in the limit $\mathcal{R} \rightarrow 1$. All the remaining cases can, in theory, still obtain, although their actual importance depends on the combination of the other physical parameters. For example, §5.4 shows how, under proper/realistic conditions, $S_{c1} + S_{c2} \xrightarrow{k_b} I_T$ and $S_{c1} + S_{c2} \xrightarrow{k_b} I_R$ could lead to significant resonant transmission and reflection respectively.

3. Regular perturbation analysis of Bragg resonance

We perform a regular perturbation analysis to solve the second- and third-order wave–bottom interaction problem in a two-layer fluid. We consider the general case in which surface-mode or internal-mode incident waves in a two-layer fluid propagate over a finite patch of periodic ripples on an otherwise uniform depth (figure 1). Following the approach of Davies (1982) who obtained a solution for the class I Bragg resonance in a one-layer fluid, we solve here the perturbed boundary-value problems (2.3) to the second order. The approach is then generalized for the third order analysis, where quartet wave resonance takes place.

For class I and class II we define reflection and transmission coefficients R_{pq} and T_{pq} , where p and q represent respectively the modes of the incident wave and the resonant wave, with $p, q = s$ or i denoting surface- or internal-mode waves respectively. Thus,

we define $R_{ss} \equiv A_s^R/a$, $R_{si} \equiv A_i^R/a$ and $T_{si} \equiv A_i^T/a$; and $R_{is} \equiv A_s^R/b$, $R_{ii} \equiv A_i^R/b$ and $T_{is} \equiv A_s^T/b$; where A_s^R and A_s^T are respectively the amplitudes of the reflected and transmitted surface-mode waves on the free surface and A_i^R and A_i^T respectively those of the reflected and transmitted internal-mode waves on the interface. For Class III, where two incident waves participate in the resonance, the first index of reflection/transmission coefficients is replaced by two, and a is the amplitude of higher amplitude incident wave; e.g. T_{iis} represents the transmission coefficient associated with a surface-mode resonant wave due to the interaction of two internal-mode incident waves with the bottom. It can be shown that theoretical results obtained in this section for those interactions without involvement of internal waves, in the limiting case of $\mathcal{R} \rightarrow 1$ (i.e. a homogeneous fluid layer), reduce to those of Davies (1982) and Liu & Yue (1998).

3.1. Class I

At $m = 1$, the solution for a right-going incident wave is (2.4). At $m = 2$, only $f_6^{(2)}$ is associated with the interaction of the incident wave and the bottom ripples, while the other inhomogeneous terms $f_j^{(2)}$, $j = 1, \dots, 5$, represent the self-interaction of the incident wave. Therefore to find the solution associated with class I resonance, we need to consider the effect of $f_6^{(2)}$ only. The system of equations (2.3) with $f_6^{(2)} \neq 0$ (and $f_j^{(2)} = 0$, $j = 1, \dots, 5$) can be solved using Fourier transform to yield the second-order potentials in the upper and lower layers in terms of Fourier integrals:

$$\phi_u^{(2)}(x, z, t) = \frac{1}{\sqrt{2\pi}} \int_{-\infty}^{\infty} \{ [A_{u1}(\xi) \cosh(\xi z) + B_{u1}(\xi) \sinh(\xi z)] \cos(\omega t) + [A_{u2}(\xi) \cosh(\xi z) + B_{u2}(\xi) \sinh(\xi z)] \sin(\omega t) \} e^{-i\xi x} d\xi, \quad (3.1)$$

$$\phi_\ell^{(2)}(x, z, t) = \frac{1}{\sqrt{2\pi}} \int_{-\infty}^{\infty} \{ [A_{\ell1}(\xi) \cosh(\xi z) + B_{\ell1}(\xi) \sinh(\xi z)] \cos(\omega t) + [A_{\ell2}(\xi) \cosh(\xi z) + B_{\ell2}(\xi) \sinh(\xi z)] \sin(\omega t) \} e^{-i\xi x} d\xi, \quad (3.2)$$

where

$$A_{uj}(\xi) = \frac{g\omega^2 \Lambda_j(\xi)}{\sqrt{2\pi} \tilde{D}(\xi, \omega)}, \quad B_{uj} = \frac{\omega^2}{g\xi} A_{uj}(\xi), \quad A_{\ell j} = A_{uj}(\xi) \hat{A}, \quad B_{\ell j} = B_{uj}(\xi) \hat{B} \quad (3.3)$$

for $j = 1$ and 2 . The coefficients $\Lambda_1(\xi)$, $\Lambda_2(\xi)$, \tilde{D} , \hat{A} and \hat{B} are defined by

$$\Lambda(\xi, t) \equiv \Lambda_1(\xi) \cos(\omega t) + \Lambda_2(\xi) \sin(\omega t) = \int_{-\infty}^{\infty} \left[\eta_{b,x} \phi_{\ell,x}^{(1)} - \eta_b \phi_{\ell,zz}^{(1)} \right]_{z=-h_u-h_\ell} e^{i\xi x} dx, \quad (3.4)$$

$$\tilde{D}(\xi, \omega) = \mathcal{D}(\xi, \omega) \sinh \xi h_u \sinh \xi h_\ell, \quad (3.5)$$

$$\hat{A} = 1 + \frac{\omega^4 - g^2 \xi^2}{2g\xi\omega^2} (1 - \mathcal{R}) \sinh 2\xi h_u, \quad (3.6)$$

$$\hat{B} = 1 - \frac{\omega^4 - g^2 \xi^2}{2\omega^4} (1 - \mathcal{R})(1 - \cosh 2\xi h_u). \quad (3.7)$$

The integrals in (3.1) and (3.2) can be evaluated by standard contour integration in terms of their residues in the complex plane (e.g. Davies 1982). For specificity, consider a right-going surface (or internal) incident wave with a wavenumber $k = k_s$ (or k_i) and frequency ω , propagating over a patch of bottom undulations, consisting of M_b ripples in the region $x = \pm L$, given by $\eta_b = d \sin(k_b x)$ for $|x| \leq L$ and $\eta_b = 0$ for

$|x| > L$, where $L = M_b \pi / k_b$. From (3.4), we obtain $\Lambda_1(\xi)$ and $\Lambda_2(\xi)$. The elevations of the reflected and transmitted surface and internal waves are (for details of derivation see Alam 2008)

$$\eta_u^{(2)}(x, t) = \omega^4 \alpha(k_s) \beta_s^R(k_s, k) \cos(k_s x + \omega t) + \omega^4 \alpha(k_i) \beta_s^R(k_i, k) \cos(k_i x + \omega t), \quad (3.8)$$

$$\eta_\ell^{(2)}(x, t) = \omega^4 \alpha(k_s) \beta_i^R(k_s, k) \cos(k_s x + \omega t) + \omega^4 \alpha(k_i) \beta_i^R(k_i, k) \cos(k_i x + \omega t), \quad (3.9)$$

as $x \rightarrow -\infty$, and

$$\eta_u^{(2)}(x, t) = \omega^4 \alpha(k_s) \beta_s^T(k_s, k) \cos(k_s x - \omega t) + \omega^4 \alpha(k_i) \beta_s^T(k_i, k) \cos(k_i x - \omega t), \quad (3.10)$$

$$\eta_\ell^{(2)}(x, t) = \omega^4 \alpha(k_s) \beta_i^T(k_s, k) \cos(k_s x - \omega t) + \omega^4 \alpha(k_i) \beta_i^T(k_i, k) \sin(k_i x - \omega t), \quad (3.11)$$

as $x \rightarrow +\infty$, where

$$\beta_i^{R,T}(\xi, k) = \beta_s^{R,T}(\xi, k) \lambda(\xi), \quad \lambda(\xi) = \cosh \xi h_u - \frac{g\xi}{\omega^2} \sinh \xi h_u, \quad \alpha(\xi) = \left(\frac{d\tilde{D}}{d\xi} \right)^{-1},$$

$$\beta_s^R(\xi, k) = (-1)^{m+1} \frac{2ad\xi k_b \lambda(k) \sin(k + \xi)L}{[(k + \xi)^2 - k_b^2] \sinh kh_\ell}, \quad (3.12)$$

$$\beta_s^T(\xi, k) = (-1)^{m+1} \frac{2ad\xi k_b \lambda(k) \sin(k - \xi)L}{[(k - \xi)^2 - k_b^2] \sinh kh_\ell}. \quad (3.13)$$

This solution shows that regardless of whether the incident wave is surface or internal mode, both surface and internal modes are present in the reflected and transmitted waves. From (3.8) to (3.11), it is clear that $A_s^R = \omega^4 \alpha(k_s) \beta_s^R(k_s, k)$, $A_i^R = \omega^4 \alpha(k_i) \beta_i^R(k_i, k)$, $A_s^T = \omega^4 \alpha(k_s) \beta_s^T(k_s, k)$ and $A_i^T = \omega^4 \alpha(k_i) \beta_i^T(k_i, k)$.

Under the class I Bragg condition, one of the reflected/transmitted surface-/internal- wave components is significantly amplified, as evidenced by vanishing of the denominator of β_s^R in (3.12) or β_s^T in (3.13). For the six cases of class I resonances, the reflection or transmission coefficient of the resonance-generated wave at the exact resonance condition is determined to be

$$R_{ss} = \frac{M_b \pi d \omega^4 \alpha(k_s) \lambda(k_s)}{2 \sinh k_s h_\ell}, \quad \text{for } k = k_s, k_b = 2k_s; \quad (3.14)$$

$$R_{si} = \frac{M_b \pi d \omega^4 \alpha(k_i) \lambda(k_s)}{\sinh k_s h_\ell} \cdot \frac{k_i}{k_i + k_s}, \quad \text{for } k = k_s, k_b = k_s + k_i; \quad (3.15)$$

$$T_{si} = \frac{M_b \pi d \omega^4 \alpha(k_i) \lambda(k_s)}{\sinh k_s h_\ell} \cdot \frac{k_i}{k_i - k_s}, \quad \text{for } k = k_s, k_b = k_i - k_s; \quad (3.16)$$

$$R_{ii} = \frac{M_b \pi d \omega^4 \alpha(k_i)}{2 \sinh k_i h_\ell}, \quad \text{for } k = k_i, k_b = 2k_i; \quad (3.17)$$

$$R_{is} = \frac{M_b \pi d \omega^4 \alpha(k_s)}{\sinh k_i h_\ell} \cdot \frac{k_s}{k_i + k_s}, \quad \text{for } k = k_i, k_b = k_s + k_i; \quad (3.18)$$

$$T_{is} = \frac{M_b \pi d \omega^4 \alpha(k_s)}{\sinh k_i h_\ell} \cdot \frac{k_s}{k_i - k_s}, \quad \text{for } k = k_i, k_b = k_i - k_s. \quad (3.19)$$

Our analysis is general for any density ratio \mathcal{R} . Before looking at ocean values of \mathcal{R} , it is of some interest to look at the perturbation theory predictions for a broader range of density ratios. In addition to theoretical interest, these are useful for comparisons with other experimental studies (Melville & Helfrich 1987, for example, use $\mathcal{R} = 0.85$) and computational (Dias & Vanden-Broeck 2003, for example, use $\mathcal{R} = 0.4, 0.5$) of

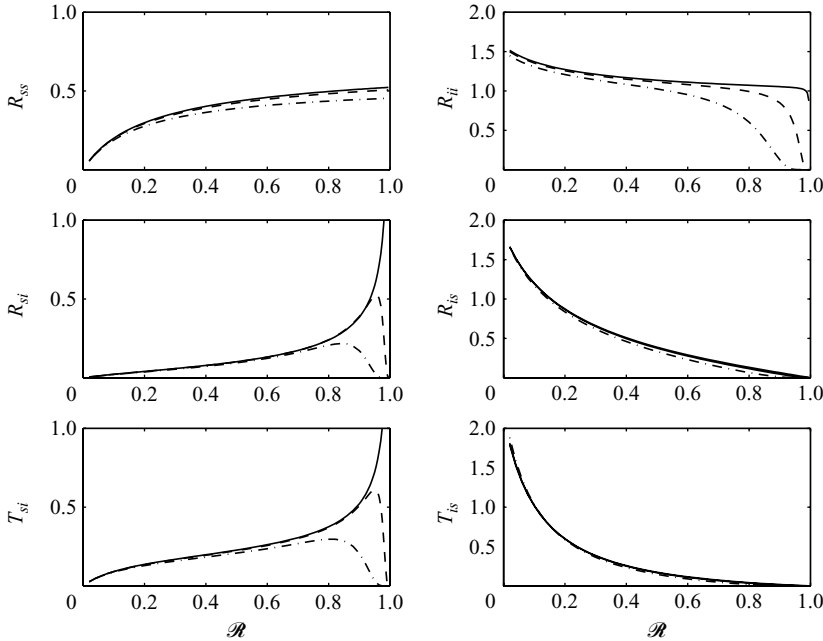


FIGURE 5. Variations of the reflection and transmission coefficients of the resonance-generated wave under the exact class I Bragg resonance condition as functions of density ratio \mathcal{R} : $d/h_\ell = 0.1$, $M_b = 20$, $h_\ell/h_u = 0.5$ and $\omega^2 h_u/g = 0.25$, $(-\cdot-)$; $\omega^2 h_u/g = 0.0625$, $(--)$; $\omega^2 h_u/g = 0.0025$ (—).

density-stratified phenomena, for applications such as two-layer tanks (Veletsos & Shivakumar 1993) and motion of dilute mud on the ocean floor (Jamali *et al.* 2003).

Figure 5 shows the variation of the maximum amplitude of the resonance-generated wave under the exact class I Bragg condition as a function of \mathcal{R} for three different dimensionless frequencies $\omega^2 h_u/g = 0.25$, 0.0625 and 0.0025 . For an upper layer depth of $h_u = 5$ m, say, these correspond to waves of periods $T = 9$ s, 18 s and 90 s respectively. The behaviors of R_{ss} , R_{is} and T_{is} are similar for different dimensionless frequencies. The reflection coefficient of the surface-mode wave R_{ss} increases as \mathcal{R} increases and approaches a finite number as $\mathcal{R} \rightarrow 1$, as in the case of a homogeneous fluid. Conversely, R_{is} and T_{is} decrease as \mathcal{R} increases and vanish at the limit of $\mathcal{R} \rightarrow 1$. Coefficients R_{si} and T_{si} behave similarly. For a relative low-frequency surface-mode incident wave, R_{si} and T_{si} always increase as \mathcal{R} increases and go unbounded as $\mathcal{R} \rightarrow 1$. For incident waves of higher frequencies, however, the increases in R_{si} and T_{si} stop at an extremum point and then decay to zero. For the resonant reflection of an internal-mode waves due to an internal-mode incident wave, R_{ii} decreases with the increase of \mathcal{R} and may reach a finite value in the limit of $\mathcal{R} \rightarrow 1$.

Figure 5 shows that the results can behave qualitatively quite differently for $1 - \mathcal{R} \sim O(1)$ or not. To illustrate some features of the former, we show in figure 6 all six cases of class I resonance as functions of relative wavenumber $2k_s/k_b$ for a fixed incident-wave frequency, where k_s is the wavenumber of the surface-mode wave for this frequency. For each resonance case, in general, the reflection or transmission coefficient of the resonant surface or internal wave obtains its maximum value at exact resonance (given by (3.14)–(3.19)) and decreases away from the resonance in a sinc manner. The surface wave has higher energy than the internal wave of the

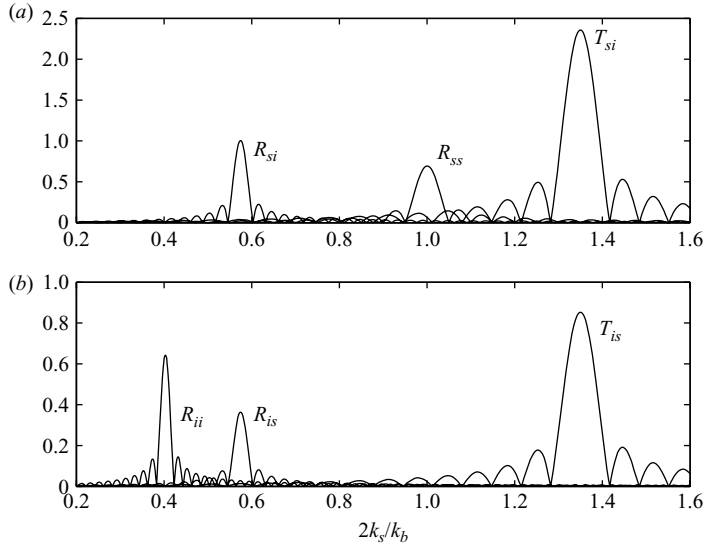


FIGURE 6. Reflection and transmission coefficients of the resonance-generated wave in the neighbourhood of class I Bragg resonance as functions of relative wavenumber $2k_s/k_b$ for (a) a surface mode and (b) an internal mode incident wave: $\mathcal{R} = 0.5$, $h_\ell/h_u = 1$, $\omega^2 h_u/g = 0.2$, $d/h_\ell = 0.1$ and $M_b = 20$. For surface-mode incident waves ($k = k_s$), R_{si} , R_{ss} and T_{si} associated with class I resonances exactly satisfied at $2k_s/k_b = 0.575$, 1.000 and 1.350 are shown in (a). For internal-mode incident waves ($k = k_i$), R_{ii} , R_{is} and T_{is} associated respectively with class I resonances exactly satisfied at $2k_s/k_b = 0.403$, 0.575 and 1.350 are shown in (b).

same height; therefore coefficients R_{si} , T_{si} are generally greater than their internal counterparts R_{is} , T_{is} .

We now turn to realistic ocean stratification of $1 - \mathcal{R} \ll 1$. In this limit, for the class I Bragg resonance to occur, in case of R_{ss}/R_{ii} , the wavelength of surface/interfacial wave is of the same order (exactly double in value) as the wavelength of the bottom waviness. From figure 5 we see that even with a weak stratification, R_{ss} can differ from that for homogeneous fluid. This is discussed in an example in §5.1. The underlying mechanism of R_{ii} reflection is the direct extension of Bragg resonance in a homogeneous fluid. It is seen that R_{ii} may remain finite as $\mathcal{R} \rightarrow 1$, which may explain the reflection of internal waves on continental shelves (§5.2).

If one surface wave and one interfacial wave participate in the resonance, then for a weak stratification, it can be shown that the wavelength of the surface wave has to be much larger than both the internal-wave and the bottom-topography wavelengths. This may not be realistic relative to typical observed field conditions. However, there are special cases such as high-frequency internal waves in lakes in which these conditions may obtain (§5.3).

From figure 5 it is seen that the coefficients R_{is} and T_{is} decrease as \mathcal{R} increases and vanish at the limit of $\mathcal{R} \rightarrow 1$. In this limit a unit-amplitude incident internal wave has zero energy and hence cannot excite a finite-amplitude surface-mode wave. Figure 5 also shows that for a relatively low-frequency incident surface-mode wave, R_{si} and T_{si} increase indefinitely in the limit of $1 - \mathcal{R} \ll 1$. These strong resonances are shown to offer possible mechanisms for the generation of high-frequency internal waves in seas and lakes (§5.3). They also provide a potential mechanism for the generation of high-amplitude very-short-wavelength internal waves (over realistic bottom ripples) that upon breaking may result in a significant vertical mixing in the water layer (Hill 2004).

3.2. Class II

Class II Bragg resonances occur at the third order and involve four wave/bottom components. Specifically, two propagating surface/internal waves and two bottom waves are involved in class II resonance. We consider the general problem of an incident wave, wavenumber k and frequency ω , propagating over a rippled bottom, consisting of two wave components with wavenumbers k_{b1} and k_{b2} . Without loss of generality, the free-surface elevation of the incident wave and bottom elevation are assumed to be

$$\eta_s^{(1)}(x, t) = a \sin(kx - \omega t), \quad \eta_b(x) = d_1 \sin(k_{b1}x) + d_2 \sin(k_{b2}x), \quad (3.20)$$

where d_1 and d_2 represent the amplitudes of the two bottom-ripple components. The objective here is to derive the solution of the third-order boundary-value problem (2.3) with $m = 3$, associated with class II resonance.

Class II resonance is governed by the third-order boundary-value problem (2.3) with $f_j^{(3)} = 0, j = 1, \dots, 5$, and $f_6^{(3)}$ given by an expression similar to (2.9f). This boundary-value problem can be solved using the same procedure in §3.1 for the class I resonance. For a patch of bottom ripples located in $|x| \leq L$, the displacements of surface and internal waves at far upstream and downstream are obtained:

$$\eta_u^{(3\mp)}(x, t) = \omega^3 \alpha(k_s) \beta_s^\mp(k_s) \cos(k_s x \pm \omega t) + \omega^3 \alpha(k_i) \beta_s^\mp(k_i) \cos(k_i x \pm \omega t), \quad (3.21)$$

$$\eta_\ell^{(3\mp)}(x, t) = \omega^3 \alpha(k_s) \beta_i^\mp(k_s) \cos(k_s x \pm \omega t) + \omega^3 \alpha(k_i) \beta_i^\mp(k_i) \cos(k_i x \pm \omega t), \quad (3.22)$$

for $x \rightarrow \mp\infty$, where

$$\beta_s^\mp(\xi) = 2a \sum_{j=1}^8 U_j \frac{\sin[(\hat{k}_j \pm \xi)L]}{\hat{k}_j \pm \xi}; \quad \beta_i^\mp(\xi) = \lambda(\xi) \beta_s^\mp(\xi); \quad (3.23)$$

where $\hat{k}_{8,1} = k \pm 2k_{b1}$, $\hat{k}_{2,3} = k - k_{b1} \pm k_{b2}$, $\hat{k}_{4,5} = k \pm 2k_{b2}$, and $\hat{k}_{6,7} = k + k_{b1} \pm k_{b2}$ and coefficients U_j are given in §A.1 of Appendix A.

For illustration, we consider a relatively simple case with a monochromatic bottom variation, and let $d_1 = d_2 = d/2$ and $k_{b1} = k_{b2} = k_b$. Let the incident wave to be a surface mode with wavenumber $k = k_s$ and frequency ω . Under the condition $k_b = (k_s + k_i)/2$, class II resonance occurs, and the resonance-generated wave is the reflected wave of internal mode. The reflection coefficient of the resonant wave is

$$R_{si} = \frac{|\eta_\ell^{(3-)}|}{|\eta_u^{(1)}|} = 2d^2 L \omega \alpha(k_i) (k_s^2 + 2k_b^2 - 3k_s k_b) \lambda(k_s) \lambda(k_i) [\sinh(k_s h_\ell) \mathcal{D}(\bar{k}_4, \omega)]^{-1} \\ \times \{ \omega^4 (\mathcal{R} \coth \bar{k}_4 h_\ell + \coth \bar{k}_4 h_u) - g \bar{k}_4 \omega^2 (1 + \coth \bar{k}_4 h_u \coth \bar{k}_4 h_\ell) \\ + g^2 \bar{k}_4^2 \coth \bar{k}_4 h_\ell (1 - \mathcal{R}) \}. \quad (3.24)$$

As expected, in class II resonance, R_{si} is independent of the incident-wave amplitude and has a quadratic dependence on the ripple amplitude and a linear dependence on the patch length.

3.3. Class III

Class III Bragg resonances, similar to Class II, occur at the third order and involve four wave/bottom components: three propagating surface/internal waves and one bottom wave are involved in class III resonance. The regular perturbation analysis for class III Bragg resonance is much more involved than those for class I and class II

resonances since all inhomogeneous terms in the third-order boundary-value problem (2.3), $f_j^{(3)}$, $j = 1, \dots, 6$, must be taken into account. We consider the general case of two incident wave components with the free-surface elevation given by

$$\eta_u^{(1)} = a_1 \sin(k_1 x - \omega_1 t) + a_2 \sin(k_2 x - \omega_2 t), \quad (3.25)$$

where a_1, a_2, k_1, k_2 and ω_1, ω_2 are respectively the amplitude, wavenumber and frequency of incident wave components 1, 2. The rippled bottom is given by $\eta_b(x) = d \sin(k_b x)$. At the second order ($m = 2$), resonance is assumed not to occur, as the interest here is in the third-order resonance, and the second-order solution of (2.3) can be readily obtained. In general, the second-order solutions for both potentials and elevations contain terms with wavenumbers $2k_1, 2k_2, k_1 \pm k_2, k_1 \pm k_b$ and $k_2 \pm k_b$. Based on the first- and second-order solutions, the forcing terms in the third-order boundary-value problem, $f_j^{(3)}$, $j = 1, \dots, 6$, can be determined.

The resulting system of equations at the third order can be solved using Fourier transform as in §3.1. The final solutions for the potentials are

$$\begin{aligned} \phi_u^{(3)}(x, z, t) = & \frac{1}{2\pi} \int_{-\infty}^{\infty} \{ [A_{u1} \cosh(\xi z) + B_{u1} \sinh(\xi z)] \cos(\omega_+ t) \\ & + [A_{u2} \cosh(\xi z) + B_{u2} \sinh(\xi z)] \sin(\omega_+ t) \} e^{-i\xi x} d\xi, \end{aligned} \quad (3.26)$$

$$\begin{aligned} \phi_\ell^{(3)}(x, z, t) = & \frac{1}{2\pi} \int_{-\infty}^{\infty} \{ [A_{\ell1} \cosh(\xi z) + B_{\ell1} \sinh(\xi z)] \cos(\omega_+ t) \\ & + [A_{\ell2} \cosh(\xi z) + B_{\ell2} \sinh(\xi z)] \sin(\omega_+ t) \} e^{-i\xi x} d\xi, \end{aligned} \quad (3.27)$$

where $\omega_+ = \omega_1 + \omega_2$. Coefficients $A_{uj}, B_{uj}, A_{\ell j}$ and $B_{\ell j}$ are given in §A.2 of Appendix A.

As an illustration of this solution, we consider a relatively simple case for which there is only one (right-going) incident-wave component, i.e. $\eta_u^{(1)} = a \sin(kx - \omega t)$. In the third-order interaction, this incident wave is counted twice, i.e. $k_1 = k_2 = k$ and $\omega_1 = \omega_2 = \omega$. Under the class III resonance condition, the resonant free-wave component with wavenumber $k_r = 2k \pm k_b$ and frequency $\omega_r = 2\omega$ is generated. Depending on the values of k and k_b , four different situations exist: the generated wave is a transmitted (or reflected) wave of surface mode if $k_r = k_{rs}$ (or $-k_{rs}$), and it is a transmitted (or reflected) wave of internal mode if $k_r = k_{ri}$ (or $-k_{ri}$). Here k_{rs} and k_{ri} are the wavenumbers of surface and internal modes associated with the frequency ω_r . The solution for the potentials associated with class III Bragg resonance is (r is removed from k subscripts for brevity)

$$\begin{aligned} \phi_u^{(3)}(x, z, t) = & \sum_{\xi=k_s, -k_s, k_i, -k_i} \text{Res}(\xi) \tilde{D}(\xi) \{ [A_{u1} \cosh(\xi z) + B_{u1} \sinh(\xi z)] \cos(\omega_r t) \\ & + [A_{u2} \cosh(\xi z) + B_{u2} \sinh(\xi z)] \sin(\omega_r t) \} e^{-i\xi x}, \end{aligned} \quad (3.28)$$

$$\begin{aligned} \phi_\ell^{(3)}(x, z, t) = & \sum_{\xi=k_s, -k_s, k_i, -k_i} \text{Res}(\xi) \tilde{D}(\xi) \{ [A_{\ell1} \cosh(\xi z) + B_{\ell1} \sinh(\xi z)] \cos(\omega_r t) \\ & + [A_{\ell2} \cosh(\xi z) + B_{\ell2} \sinh(\xi z)] \sin(\omega_r t) \} e^{-i\xi x}. \end{aligned} \quad (3.29)$$

Coefficients of the potential in this special case can be expressed in a closed form (see Alam 2008). It then can be shown that

$$[(iA_{u2} - A_{u1})\tilde{D}]|_{\xi=-k_x} = [(-iA_{u2} - A_{u1})\tilde{D}]|_{\xi=k_x} \equiv \beta(k_x) \text{ for } x = i, s. \quad (3.30)$$

Thus, we have at far upstream ($x \rightarrow -\infty$)

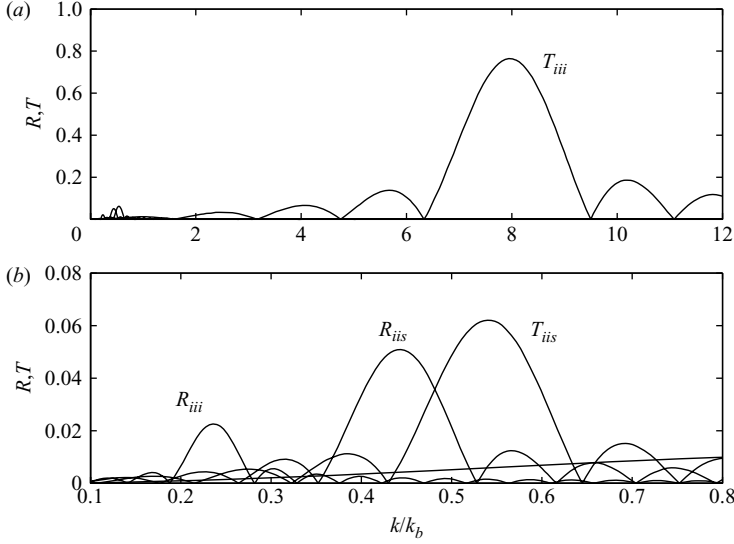


FIGURE 7. Reflection and transmission coefficients of resonant surface and internal waves in the neighbourhood of class III Bragg resonance for a single surface incident wave over a rippled bottom. The parameters are $h_\ell/h_u = 1$, $\mathcal{R} = 0.96$, $kh_u = 0.3$ ($\omega^2 h_u/g = 0.02$), $ka = 0.06$, $kd = 0.001$ and $M_b = 5$; (b) is a close-up of (a) for small k/k_b .

$$\phi_u^{(3-)}(x, 0, t) = \beta_i \alpha(k_i) \sin(k_i x + \omega_r t) + \beta_s \alpha(k_s) \sin(k_s x + \omega_r t), \quad (3.31)$$

$$\eta_u^{(3-)}(x, t) = \frac{\omega_r}{g} [\beta_i \alpha(k_i) \cos(k_i x + \omega_r t) + \beta_s \alpha(k_s) \cos(k_s x + \omega_r t)], \quad (3.32)$$

$$\eta_\ell^{(3-)}(x, t) = \frac{\omega_r}{g} [\beta_i \lambda(k_i) \alpha(k_i) \cos(k_i x + \omega_r t) + \beta_s \lambda(k_s) \alpha(k_s) \cos(k_s x + \omega_r t)] \quad (3.33)$$

and

$$R_{iis} = \frac{|\eta_u^{(3-)}|}{|\eta_\ell^{(1)}|}, \quad R_{iii} = \frac{|\eta_\ell^{(3-)}|}{|\eta_\ell^{(1)}|}. \quad (3.34)$$

Transmission coefficients T_{iis} , T_{iii} are derived similarly. As an illustration, we consider a problem with the following parameters: $h_\ell/h_u = 1$, $\mathcal{R} = 0.96$, $kh_u = 0.3$ ($\omega^2 h_u/g = 0.02$), $ka = 0.06$, $kd = 0.001$ and $M_b = 5$. For an internal incident wave, class III resonances occur at (i) $k/k_b = 7.9$ with a resonant transmitted internal wave; (ii) $k/k_b = 0.24$ with a resonant reflected internal wave; (iii) $k/k_b = 0.44$ with a resonant reflected surface wave; and (iv) $k/k_b = 0.54$ with a resonant transmitted surface wave. Figure 7 shows the reflection and transmission coefficients of the resonant waves for all four cases of class III resonance when the incident wave has only one component. We remark that the case for two different incident waves can be worked out in a similar way. The algebra is much more tedious and the formulas quite lengthy and are not presented here.

4. Multiple-scale analysis for class I Bragg resonance

The regular perturbation solution derived in the preceding section is valid only for resonant interactions bounded in their growth spatially by the length of the bottom topography. The reflection and transmission coefficients of the resonant wave predicted by (3.14) to (3.19) increase linearly with the number of bottom ripples M_b

(or, equivalently, the length of the bottom patch $2L$), violate energy conservation and are clearly invalid for $M_b, L \rightarrow \infty$. To obtain a uniformly valid solution, we apply here a multiple-scale analysis of class I Bragg resonance following the approach of Mei (1985). Our objective is to obtain and elucidate the solution for the resonance cases presented in §2.2.

We consider the interaction of a surface/internal wave with bottom ripples in the neighbourhood of class I Bragg resonance. We introduce slow variables $\bar{x} = \epsilon x$ and $\bar{t} = \epsilon t$ and make multiple-scale expansions for the potentials in the two fluid layers:

$$\phi_u = \epsilon \phi_u^{(1)} + \epsilon^2 \phi_u^{(2)} + O(\epsilon^3) \quad \text{and} \quad \phi_\ell = \epsilon \phi_\ell^{(1)} + \epsilon^2 \phi_\ell^{(2)} + O(\epsilon^3), \quad (4.1)$$

where $\phi_u^{(1)}$, $\phi_\ell^{(1)}$, $\phi_u^{(2)}$ and $\phi_\ell^{(2)}$ are all functions of fast variables, x , z and t , and slow variables, \bar{x} and \bar{t} . Upon substitution of the multiple-scale asymptotic expansion of (4.1) into the governing equations (2.1) and collecting the same-order terms, at the first order the linear result of (2.4) is retrieved. At the second order applying the solvability condition gives rise to two partial differential equations governing the amplitude of the incident wave (A) and the amplitude of resonant wave (A^r) on the free surface. The derivation is the extension of Mei (1985) to two layer and is given in Alam (2008). Partial differential equations governing the amplitude evolutions are

$$A_{,\bar{t}} + C_g A_{,\bar{x}} + \mathcal{M} A^r = 0 \quad \text{and} \quad (4.2)$$

$$A^r_{,\bar{t}} + C_g^r A^r_{,\bar{x}} + \mathcal{N} A = 0, \quad (4.3)$$

where C_g and C_g^r are the group velocities of the incident and resonance-generated waves respectively and

$$\begin{aligned} \mathcal{M} = & \omega^3 d \lambda \lambda^r k \sinh kh_\ell / (2\mathcal{R} g k \sinh kh_\ell - 3\mathcal{R} \lambda g k \sinh kh_\ell \cosh kh_u \\ & + 3\mathcal{R} \lambda \omega^2 \sinh kh_\ell \sinh kh_u + \mathcal{R} g \lambda^2 k \sinh kh_\ell + 3\omega^2 \lambda^2 \cosh kh_\ell \\ & - g \lambda^2 k \sinh kh_\ell) / (2 \sinh kh_\ell \sinh k^r h_\ell), \end{aligned}$$

$$\begin{aligned} \mathcal{N} = & \omega^3 d \lambda \lambda^r k^r \sinh k^r h_\ell / (2\mathcal{R} g k^r \sinh k^r h_\ell - 3\mathcal{R} \lambda^r g k^r \sinh k^r h_\ell \cosh k^r h_u \\ & + 3\mathcal{R} \lambda^r \omega^2 \sinh k^r h_\ell \sinh k^r h_u + \mathcal{R} g \lambda^r k^r \sinh k^r h_\ell + 3\omega^2 \lambda^r \cosh k^r h_\ell \\ & - g \lambda^r k^r \sinh k^r h_\ell) / (2 \sinh kh_\ell \sinh k^r h_\ell), \end{aligned}$$

with $\lambda = \cosh(kh_u) - (gk/\omega^2) \sinh(kh_u)$ and $\lambda^r = \cosh(k^r h_u) - (gk^r/\omega^2) \sinh(k^r h_u)$. Here k and ω are the wavenumber and frequency of the (right-going) incident wave and k^r is the wavenumber of the resonance-generated wave given by the class I Bragg resonance condition: $k^r = k \pm k_b$.

Combining (4.2) and (4.3), we obtain two decoupled partial differential equations for A and A^r :

$$\left[\frac{\partial^2}{\partial \bar{t}^2} + C_g C_g^r \frac{\partial^2}{\partial \bar{x}^2} + (C_g + C_g^r) \frac{\partial^2}{\partial \bar{x} \partial \bar{t}} - \mathcal{M} \mathcal{N} \right] \begin{Bmatrix} A \\ A^r \end{Bmatrix} = 0. \quad (4.4)$$

In the following, we focus on long-scale variations only, and, for clarity, all overbars on x and t are omitted hereafter in this section.

For the steady solution, A and A^r are independent of t , and (4.4) becomes

$$\left(\frac{\partial^2}{\partial x^2} - \frac{\mathcal{M} \mathcal{N}}{C_g C_g^r} \right) \begin{Bmatrix} A \\ A^r \end{Bmatrix} = 0. \quad (4.5)$$

For the case in which the resonance-generated wave is a transmitted wave (i.e. $k^r = k_s$ or k_i), it can be shown that $\kappa^2 \equiv -\mathcal{M}\mathcal{N}/(C_g C_g^r) > 0$. In this case the solution is

$$A(x) = a \cos(\kappa x), \quad A^T(x) = -\frac{\mathcal{N}}{\kappa C_g^r} a \sin(\kappa x). \quad (4.6)$$

For the case in which the resonance-generated wave is reflected (i.e. $k^r = -k_s$ or $-k_i$), it can be shown that $-\mathcal{M}\mathcal{N}/(C_g C_g^r) < 0$. Therefore by defining $\kappa^2 = \mathcal{M}\mathcal{N}/(C_g C_g^r)$ the solution takes the form

$$A(x) = a \frac{\cosh \kappa(2L - x)}{\cosh 2\kappa L}, \quad A^R(x) = a \frac{\mathcal{N}}{\kappa C_g^r} \frac{\sinh \kappa(2L - x)}{\cosh 2\kappa L}. \quad (4.7)$$

We note that in the special case of one fluid (i.e. $\mathcal{B} = 1$), the above results reduce directly to (3.5) and (3.6) of Mei (1985).

If the incident wave is detuned, i.e. it has a wavenumber of $k + \epsilon K$ and the frequency $\omega + \epsilon \Omega$, where $\mathcal{D}(k, \omega) = 0$ and $\Omega = C_g K$, then on the rippled bottom region ($0 \leq x \leq 2L$), it can be shown that

$$(A, A^r) = a [F(x), F^r(x)] e^{-i\Omega t}. \quad (4.8)$$

If the resonant generated wave is transmitted over the rippled bottom, then

$$F(x) = e^{i\mathcal{B}\Omega x} \left[-i \frac{\Omega}{2\kappa} \left(\frac{1}{C_g^r} + \frac{1}{C_g} \right) \sin(\kappa x) + \cos(\kappa x) \right], \quad (4.9a)$$

$$F^T(x) = -e^{i\mathcal{B}\Omega x} \frac{\mathcal{N}}{\kappa C_g^r} \sin(\kappa x), \quad (4.9b)$$

where

$$\mathcal{B} \equiv \frac{1}{2} \left(\frac{1}{C_g^r} - \frac{1}{C_g} \right), \quad \Omega_0 \equiv 2 \frac{|\mathcal{M}\mathcal{N}C_g C_g^r|^{\frac{1}{2}}}{|C_g - C_g^r|} \quad \text{and} \quad \kappa = \mathcal{B} (\Omega_0^2 + \Omega^2)^{1/2}.$$

If the resonance-generated wave is reflected, then for $|\Omega| < \Omega_0$

$$F(x) = \frac{e^{i\mathcal{B}\Omega x}}{\gamma^+ - \lambda^+ e^{4\kappa L}} [\gamma^+ e^{\kappa x} - \lambda^+ e^{\kappa(4L-x)}], \quad F^R(x) = \frac{e^{i\mathcal{B}\Omega x}}{\gamma^+ - \lambda^+ e^{4\kappa L}} [e^{\kappa x} - e^{\kappa(4L-x)}], \quad (4.10a)$$

where $\kappa = \mathcal{B}(\Omega_0^2 - \Omega^2)^{1/2}$, $\gamma^+ = (i\Omega - r_1 C_g^r)/\mathcal{N}$ and $\lambda^+ = (i\Omega - r_2 C_g^r)/\mathcal{N}$, and for $|\Omega| > \Omega_0$

$$F(x) = \left[1 + \frac{i\Omega (C_g^r \mathcal{B} - 1)}{\hat{\mathcal{B}}} x \right] e^{i\mathcal{B}\Omega x}, \quad F^R(x) = \frac{\mathcal{N}(2L - x)}{\hat{\mathcal{B}}} e^{i\mathcal{B}\Omega x}, \quad (4.11a)$$

where $\hat{\mathcal{B}} = C_g^r + i\Omega(L - \mathcal{B}C_g^r)$. Details of derivations are given in Appendix B.

Figure 8 compares the results of the resonant reflection or transmission coefficient in the neighbourhood of the class I Bragg resonance obtained, using the regular perturbation analysis and the multiple-scale approach. Similar result is also obtained by using the McKee (1996) approach which is based of the modified mild-slope theory of Kirby (1986). These are also shown in figure 8. All six class I resonance cases are considered. Two bottom-ripple amplitudes $d/h_u = 0.1$ and $d/h_u = 0.03$ are used. Other parameters used are $\mathcal{B} = 0.96$, $h_\ell/h_u = 0.25$, $\omega^2 h_u/g = 0.14$ and $M_b = 20$. For small-bottom-ripple amplitude, two solutions agree with each other. For

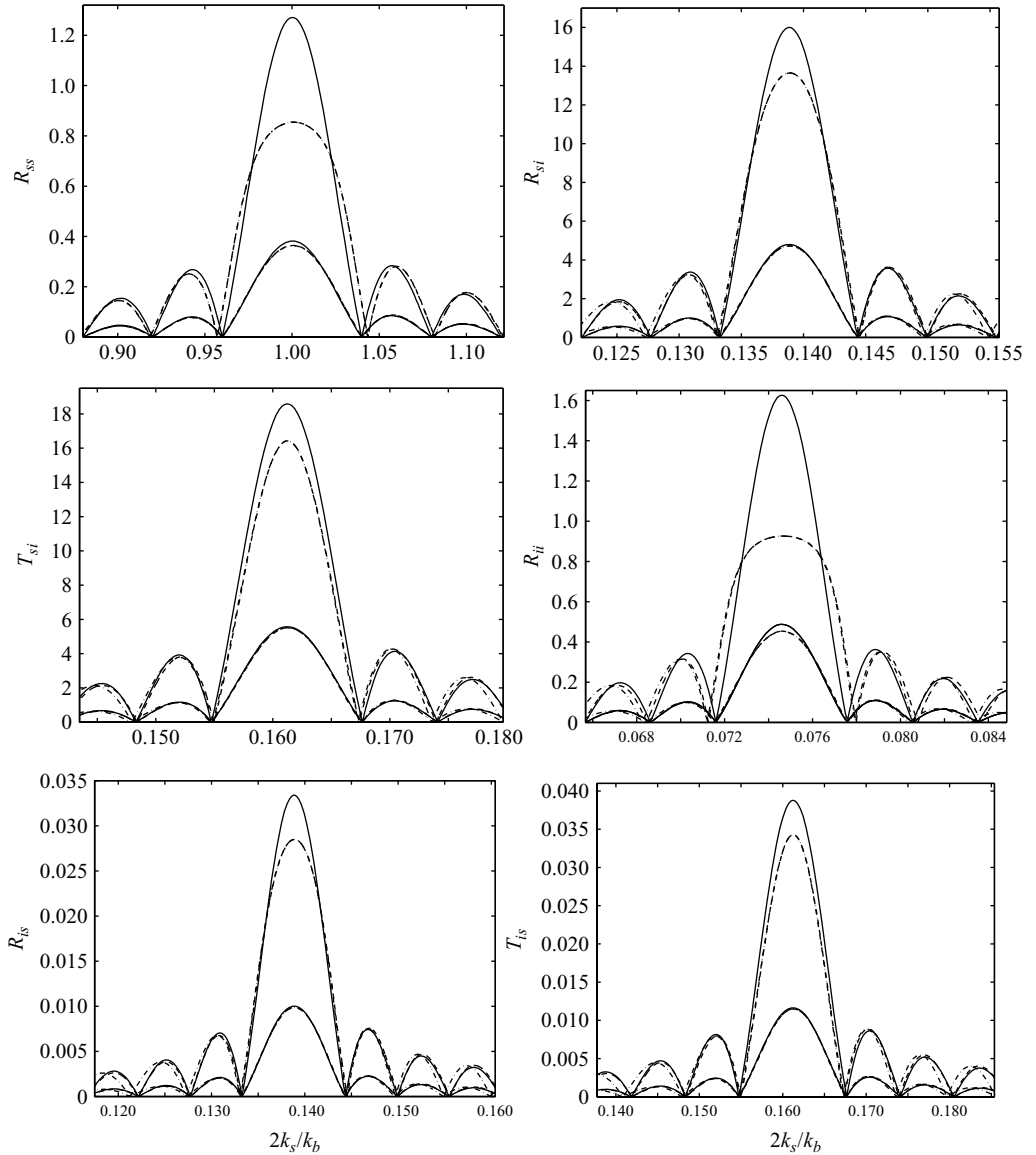


FIGURE 8. Reflection and transmission coefficients of the resonance-generated wave due to class I Bragg resonance obtained from regular perturbation theory (—); the modified mild-slope equation (---) and the multiple-scale method (-·-). (The latter two are distinguishable only far away from exact resonance.) Two bottom-rippled amplitudes are considered: $d/h_u=0.1$ and $d/h_u=0.03$. The other parameters are $\mathcal{R}=0.96$, $h_\ell/h_u=0.25$, $\omega^2 h_u/g=0.14$ and $M_b=25$.

large-bottom-ripple amplitude, the regular perturbation solution overestimates the reflection and transmission coefficients of the resonant wave.

5. Illustrative case studies

The Bragg resonance mechanisms involving two-layer density stratification and a rippled bottom discussed in the previous sections have important effects on the

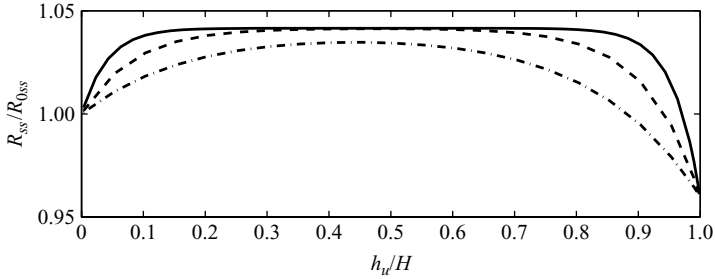


FIGURE 9. Effect of stratification on the reflection coefficient of homogeneous-fluid class I Bragg resonance. Parameters are $\mathcal{R} = 0.96$, $d/a = 1$ and $\omega^2 H/g = 3$ (- · -), $\omega^2 H/g = 6$ (- -) and $\omega^2 H/g = 12$ (—) (which in physical domain correspond to a $T = 8$ s wave travelling over a sea of respectively $H = 50$ m, 100 m, 200 m depth).

evolution of ocean waves under the appropriate conditions. We discuss four specific examples of these: the effect of stratification on classical second-order homogeneous-fluid Bragg resonance (§ 5.1); strong reflection of internal gravity waves by bottom ripples (§ 5.2); generation of high-frequency internal waves by long surface waves over bottom topography (§ 5.3); and new quartet resonances involving class III Bragg interactions among three free waves and a bottom undulation in the presence of density stratification (§ 5.4).

5.1. Modification of homogeneous-fluid class I Bragg resonance in the presence of stratification

Bragg resonance in a homogeneous fluid is well understood theoretically and experimentally (Mei 1985; Belzons, Guazzelli & Parodi 1988; Liu & Yue 1998; Ardhuin & Herbers 2002; Ardhuin & Magne 2007). Here we show that ocean stratification can significantly affect the expected homogeneous-fluid reflection coefficient. Figure 9 shows the change in the class I Bragg reflection coefficient with or without density stratification. Results are shown for $\mathcal{R} = 0.96$ for different total depths $\omega^2 H/g$ with varying thermocline depths h_u/H . Denoting the homogeneous-fluid reflection coefficient R_{0ss} , we note that R_{ss}/R_{0ss} approaches 1 as $h_u/H \rightarrow 0$, is greater than 1 for intermediate values of h_u/H and decreases below 1 for h_u/H near 1. The effect is somewhat diminished for longer incident waves (relative to total depth). The change due to the presence of stratification depends in general on \mathcal{R} , $\omega^2 H/g$, h_u/H and d/a . For the parameters chosen in figure 9, the overall effect is relatively weak (of the order of $\pm 5\%$).

5.2. Bragg reflection of internal waves

Similar to the reflection of surface waves on a homogeneous fluid, bottom ripples can strongly reflect incident internal waves. Figure 10 shows the reflection coefficient R_{ii} due to class I Bragg resonance ($I_c \xrightarrow{k_b} I_R$) for $\mathcal{R} = 0.96$, $h_\ell/h_u = 0.2$, $\omega^2 h_u/g = 0.12$, $d/h_u = 0.1$ and $M_b = 20$. For stratified layer depths of $h_u = 200$ m and $h_\ell = 40$ m, say, the chosen parameters correspond to relatively short incident internal-mode waves of wavelength $\lambda_i = 200$ m and not atypical bottom ripple wavelength of $\lambda_b = 100$ m (Guazzelli, Rey & Belzons 1991; Mei, Stiassnie & Yue 2005). Figure 10 shows that over a distance of about 2 km ($M_b = 20$), a reflected internal wave of 60% of the incident amplitude can be expected. Systematic study varying the physical parameters (Alam 2008) shows that \mathcal{R}_{ii} is generally greater for longer interfacial waves, shallower lower layer depth and stronger stratification.

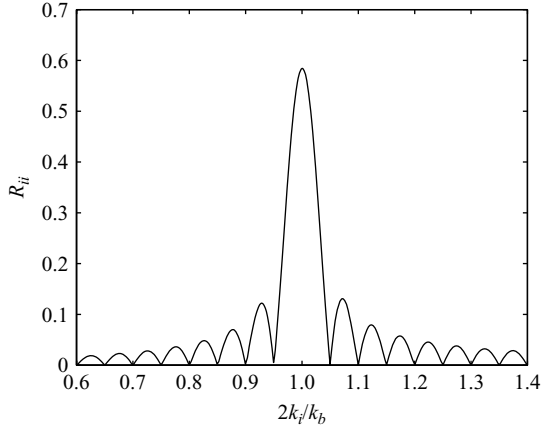


FIGURE 10. Reflection coefficients (R_{ii}) of an internal-mode resonance-generated wave in the neighbourhood of class I Bragg resonance as functions of relative wavenumber $2k_i/k_b$: $\mathcal{R} = 0.96$, $h_\ell/h_u = 0.2$, $\omega^2 h_u/g = 0.12$, $d/h_u = 0.1$ and $M_b = 20$.

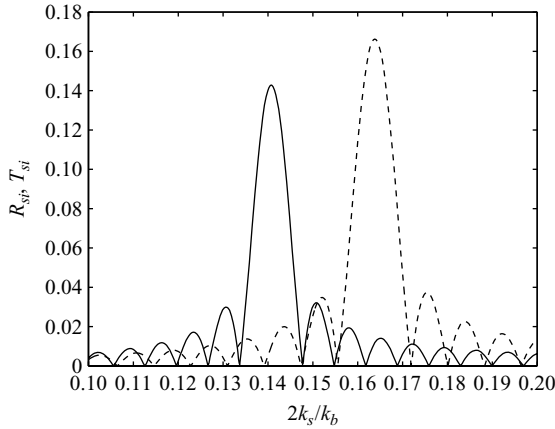


FIGURE 11. Reflection (—) and transmission (---) coefficients (R_{si} , T_{si}) for an incident surface-mode wave (wavenumber k_s) that resonate an internal-mode wave in the neighbourhood of class I Bragg resonance, as a function of relative wavenumber $2k_s/k_b$. $\mathcal{R} = 0.96$, $h_\ell/h_u = 0.5$, $\omega^2 h_u/g = 0.04$, $d/h_\ell = 0.5$ and $M_b = 20$.

5.3. Generation of high-frequency internal waves by long surface waves

High-frequency internal waves are frequently observed in lakes and coastal waters (Garrett & Munk 1975). Although many different generation mechanisms have been proposed (e.g. Thorpe *et al.* 1996), the precise origin of these waves is still a matter of current investigation (e.g. Boegman *et al.* 2003). The elucidation of internal-wave Bragg resonance here offers another possible explanation. We show here that resonant short internal waves can be generated by the interaction of very long surface wave (such as seiches in lakes) with bottom topography.

Figure 11 shows an example of generation of high-frequency internal waves due to Bragg resonance of long incident surface waves ($S_c \xrightarrow{k_{b1}} I_R$ and $S_c \xrightarrow{k_{b2}} I_T$). Parameters chosen are $\mathcal{R} = 0.96$, $h_\ell/h_u = 0.5$, $\omega^2 h_u/g = 0.04$, $d/h_\ell = 0.5$ and $M_b = 20$. These may correspond to, for example, total and thermocline depths of $H = 75$ m and $h_u = 50$ m,

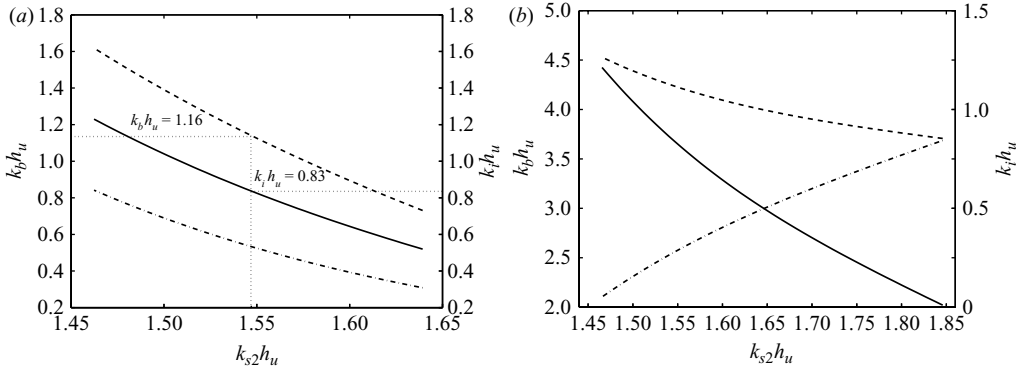


FIGURE 12. Class III Bragg resonance involving two (a) co-propagating and (b) counter-propagating, surface-mode waves (wavenumbers k_{s1} , k_{s2}); an internal-mode wave (wavenumber k_i); and a bottom-ripple component (wavenumber k_b). The physical parameters are $\mathcal{R} = 0.96$, $h_\ell/h_u = 2.3$ and, for specificity, $k_{s1}h_u = 1.85$. Given k_{s2} (bottom axis), say, the resonance curves corresponding to co-propagating ($- \cdot -$) or counter-propagating ($- - -$) internal-mode waves (relative to k_{s1}) allow one to obtain the two resonant values of k_b (left axis), while the resonant curve represented by $—$ obtains the (unique) resonant value of k_i (right axis).

surface wave of wavelength $\lambda_{in} = 2$ km and short resonant internal waves of period $T = 70$ s. In this example the resonance is relatively selective; however, it is strong. The strength, as before, increases as the length of the bottom patch increases.

5.4. Class III Bragg resonance among surface and internal waves

In the absence of bottom topography, Ball (1964), Wen (1995a), Hill & Foda (1996) and Jamali (1998) studied the triad resonance involving one internal and two surface waves and one surface and two internal waves, respectively. For realistically weak ocean stratification with $1 - R \ll 1$, such triad resonances are highly selective. In the former, the only case involves two oppositely travelling surface waves of very close wavelengths resonant with an internal wave of half the wavelength. In the latter, the two internal waves have to be oppositely travelling and of almost the same wavelength, now resonant with a surface wave of half the period.

Unlike the above, if bottom ripples are present, resonance involving three surface/internal waves obtains for a broad range of conditions under class III Bragg resonance. In particular, these conditions include co-propagating waves (as well as counter-propagating waves) and cover realistic cases of long wavelength and period internal waves relative to surface waves. Figure 12 shows the different possibilities of surface, internal and bottom wavenumbers for class III Bragg resonance involving two incident surface-mode waves (k_{s1} , k_{s2}), an internal-mode wave (k_i) and a bottom topography with component (k_b), for $\mathcal{R} = 0.96$ and $h_\ell/h_u = 2.3$ (i.e. $S_{c1} \pm S_{c2} \xrightarrow{k_{b1}} I_R$ and $S_{c1} \pm S_{c2} \xrightarrow{k_{b2}} I_T$). The cases involving (a) co-propagating and (b) counter-propagating surface waves are shown separately, and in the former case, the resonant internal wave can be co- or counter-propagating. If two incident waves are co-propagating, both of k_b s and k_i decrease as $|k_{s1} - k_{s2}|$ increases, while if two incident waves are counter-propagating, as $|k_{s1} - k_{s2}|$ increases, k_i decreases, but one of k_b s (associated with resonant internal wave that co-propagates with k_{s1}) increases. Since the stratification is weak, the depth of thermocline has a small effect on the resonance condition.

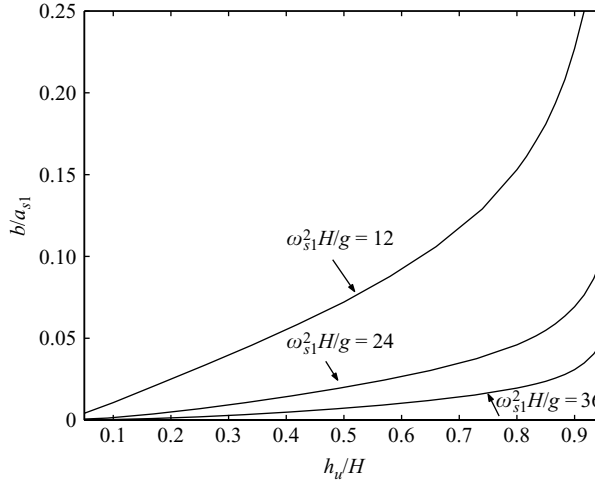


FIGURE 13. Effect of total depth of sea and the depth of thermocline on the growth rate b of internal-wave generation under class III Bragg resonance. Parameters are $\mathcal{R} = 0.96$ and two co-propagating incident surface waves $a_{s2}/a_{s1} = 1.2$, $d/a_{s1} = 6.5$, $ka_{s1} = 0.2$.

For example results for thermoclines of $h_\ell/h_u = 2.3$ and $h_\ell/h_u = 0.4$ are barely distinguishable.

For illustration, for the fixed value $k_{s1}h_u = 1.85$ ($\omega_{s1}^2 h_u/g = 1.9$), figure 12(a) shows that for a chosen value of co-propagating $k_{s2}h_u = 1.55$, bottom components of wavenumber $k_b h_u = 1.16$ resonate a counter-propagating internal wave of $k_i h_u = 0.83$. In dimensional values, for a total depth of $H = 100\text{ m}$ ($h_u = 30\text{ m}$), say, these correspond to two co-propagating incident surface waves of wavelengths $\lambda_{s1} \approx 102\text{ m}$ and $\lambda_{s2} \approx 122\text{ m}$ (corresponding periods of $T_1 \approx 8\text{ s}$, $T_2 \approx 8.8\text{ s}$), bottom wavelength of $\lambda_b \approx 116\text{ m}$, and resonant internal wave of wavelength $\lambda_i \approx 226\text{ m}$.

The rate of growth b of the class III Bragg resonant internal wave with two incident surface waves and one bottom component can be obtained by regular perturbation. The closed-form formula for the growth rate b is similar to (3.34) but is more complicated and algebraically lengthy and is not given here. Figure 13 shows the value of b for different total and thermocline depths for the $S_{c1} + S_{c2} \rightarrow I_R$ class III Bragg resonance. This resonance is stronger if the thermocline is closer to the bottom and if the sea is shallower. From regular perturbation analysis, the growth rate is linearly proportional to the amplitude of incident waves and the bottom topography (cf. (3.34)). For a thermocline close to the free surface, b increases almost linearly with h_u , whereas as $h_u/H \rightarrow 1$, b increases exponentially. For given h_u/H , b also increases rapidly as the incident wave period increases.

6. Conclusion

In this paper the generalized two-dimensional Bragg resonance of waves in a two-layer density-stratified fluid over a rippled bottom is studied analytically using perturbation theory.

Bragg resonances obtain involving triad (class I) and quartet (class II and class III) interactions at the second and third orders (in wave/bottom steepness) respectively in which at least one of the participants is a component of the rippled bottom. The results are a generalization of the unstratified (single layer) fluid case of Liu &

Yue (1998) but, because of the possibility of internal mode waves, now admit many (new) resonance cases and combinations. These are enumerated and represented schematically in Feynman-like diagrams. In class I and class II Bragg resonances only one frequency exists, while in the class III Bragg resonance, the frequency of resonant wave can be the sum or the difference of frequency of incident waves resulting in the possibility for the generation of very long or short waves. For all three classes of resonances, we obtain regular perturbation solutions which predict the resonances and the growth of the resonant transmission or reflection waves for a finite-bottom patch. For very long bottom patches, regular perturbation results are not valid, and analyses involving slow variables and multiple scales are needed. This is obtained here for the case of class I resonance.

It is shown via illustrative examples that these Bragg resonances offer new mechanisms for generation and reflection of surface and internal ocean waves under proper realistic conditions. In particular, a triad of surface/internal waves can be resonated through their interaction with bottom undulations under relatively broad class III Bragg resonance conditions.

The analysis provided in this paper is limited to two-dimensional cases. Extensions of the current analyses to three dimensions are straightforward in principle but algebraically more involved. For class I, one can show that the resonance weakens as we depart from normal incident (Alam 2008). This is also the case for a homogeneous fluid layer for class I Bragg resonance (Liu & Yue 1998). For class II and class III resonances, this may not be true in general. In the case of a single fluid layer on bottom ripples, oblique resonance in some class II and class III Bragg cases are known to be more important than that under normal incidence (Liu & Yue 1998). For two-layer density-stratified fluid without bottom variations, oblique triad resonance involving two surface and one interfacial wave and that involving two interfacial and one surface wave are, under some conditions, also known to be more important than the case of normal incidence (Hill & Foda 1998). The general case of multi-layer higher order Bragg resonance in three dimensions is an interesting extension for further investigation.

The present work provides the analytic basis and guidance for understanding the complex resonant interactions involving surface/internal mode waves travelling over a rippled bottom. In practice, the general problem consists of surface/internal mode waves and bottom topography containing multiple (indeed a spectrum of) components, plus resonant generated wave components, obtaining multiple resonances and resonant combinations among these components. For this general problem, a direct numerical simulation of the nonlinear evolution is needed. This is the subject of part II of this work (Alam *et al.* 2008).

This research is supported financially by grants from the Office of Naval Research.

Appendix A. Regular perturbation coefficients of class II and class III Bragg resonance

A.1. Class II coefficients

The coefficients U_j , $j = 1, \dots, 8$ in (3.23) are

$$\begin{aligned}
 U_1 &= -1/2 d_1 D_2 k^2 - d_1 D_2 k_{b1}^2 + 3/2 d_1 D_2 k k_{b1}, \\
 U_2 &= (1/2 d_2 D_2 - 1/2 d_1 D_3) k^2 + (1/2 d_2 k_{b2} D_2 - d_2 D_2 k_{b1} + 1/2 d_1 k_{b1} D_3 - d_1 D_3 k_{b2}) k \\
 &\quad + 1/2 (k_{b1} - k_{b2}) (d_2 D_2 k_{b1} + d_1 D_3 k_{b2}),
 \end{aligned}$$

$$U_3 = (-1/2 d_2 D_2 - 1/2 d_1 D_4) k^2 + (d_2 D_2 k_{b1} + d_1 D_4 k_{b2} + 1/2 d_1 k_{b1} D_4 + 1/2 d_2 k_{b2} D_2) k - 1/2 (k_{b2} + k_{b1}) (d_2 D_2 k_{b1} + d_1 D_4 k_{b2}),$$

$$U_4 = 1/2 d_2 D_3 k^2 + d_2 D_3 k_{b2}^2 + 3/2 d_2 D_3 k k_{b2},$$

$$U_5 = -d_2 k_{b2}^2 D_4 - 1/2 d_2 D_4 k^2 + 3/2 d_2 k_{b2} D_4 k,$$

$$U_6 = (1/2 d_2 D_1 + 1/2 d_1 D_3) k^2 + (d_1 D_3 k_{b2} + d_2 D_1 k_{b1} + 1/2 d_1 k_{b1} D_3 + 1/2 d_2 k_{b2} D_1) k + 1/2 (k_{b2} + k_{b1}) (d_2 D_1 k_{b1} + d_1 D_3 k_{b2}),$$

$$U_7 = (-1/2 d_2 D_1 + 1/2 d_1 D_4) k^2 + (-d_2 D_1 k_{b1} - d_1 D_4 k_{b2} + 1/2 d_1 k_{b1} D_4 + 1/2 d_2 k_{b2} D_1) k - 1/2 (k_{b1} - k_{b2}) (d_2 D_1 k_{b1} + d_1 D_4 k_{b2}),$$

$$U_8 = d_1 k_{b1}^2 D_1 + 3/2 d_1 k_{b1} D_1 k + 1/2 d_1 D_1 k^2,$$

where

$$D_j = -q_j [\omega^4 (\mathcal{R} \coth \bar{k}_j h_\ell + \coth \bar{k}_j h_u) - g \bar{k}_j \omega^2 (1 + \coth \bar{k}_j h_u \coth \bar{k}_j h_\ell) + g^2 \bar{k}_j^2 \coth \bar{k}_j h_\ell (1 - \mathcal{R})] / \mathcal{D}(\bar{k}_j, \omega),$$

$$q_j = \frac{\omega \bar{d}_j \lambda(k)}{2 \sinh(k h_\ell)}, \quad \lambda(\xi) = \cosh(\xi h_u) - \frac{gk}{\omega^2} \sinh(\xi h_u)$$

for $j = 1, \dots, 4$, and $\bar{k}_{1,2} = k \pm k_{b1}$, $\bar{k}_{3,4} = k \pm k_{b2}$, $\bar{d}_{1,2} = \pm d_1$ and $\bar{d}_{3,4} = \pm d_2$.

A.2. Class III coefficients

Coefficients of the third-order solution under class III Bragg resonance ((3.26) and (3.27)) are obtained by satisfying boundary conditions and are given by

$$A_{uj} \tilde{D} = (\Lambda_{4j} g - s_u^\xi s_\ell^\xi \mathcal{R} \Lambda_{1j} + c_\ell^\xi g \Lambda_{3j} - c_\ell^\xi c_u^\xi \Lambda_{1j}) \omega_+^2 - \xi s_\ell^\xi g (\Lambda_{3j} g + \mathcal{R} c_u^\xi \Lambda_{1j} - \Lambda_{2j} - c_u^\xi \Lambda_{1j}),$$

$$B_{uj} \tilde{D} = \frac{(\Lambda_{4j} + c_\ell^\xi \Lambda_{3j}) \omega_+^4}{\xi} + (s_\ell^\xi \Lambda_{2j} - s_\ell^\xi \mathcal{R} c_u^\xi \Lambda_{1j} - g s_\ell^\xi \Lambda_{3j} - \Lambda_{1j} c_\ell^\xi s_u^\xi) \omega_+^2 - \Lambda_{1j} s_u^\xi g \xi s_\ell^\xi (\mathcal{R} - 1),$$

$$A_{\ell j} \tilde{D} \xi = -s_u^\xi (s_u^\xi s_\ell^\xi \Lambda_{3j} \mathcal{R} + c_\ell^\xi c_u^\xi \Lambda_{3j} \mathcal{R} - \Lambda_{4j} c_u^\xi + c_u^\xi \Lambda_{4j} \mathcal{R}) \omega_+^4 - \xi (-s_u^\xi s_\ell^\xi c_u^\xi \Lambda_{2j} - c_\ell^\xi c_u^\xi s_u^{\xi 2} \mathcal{R} \Lambda_{1j} - s_\ell^\xi \mathcal{R} \Lambda_{1j} s_u^{\xi 3} + s_u^{\xi 2} \Lambda_{4j} g + c_\ell^\xi c_u^{\xi 3} \mathcal{R} \Lambda_{1j} - c_\ell^\xi c_u^{\xi 2} \Lambda_{2j} - \Lambda_{4j} c_u^{\xi 2} g + s_u^\xi c_u^{\xi 2} s_\ell^\xi \mathcal{R} \Lambda_{1j}) \omega_+^2 - g s_u^\xi \xi^2 (-c_\ell^\xi c_u^\xi g \Lambda_{3j} \mathcal{R} + c_\ell^\xi c_u^\xi \Lambda_{2j} + s_u^\xi s_\ell^\xi \Lambda_{2j} - s_u^\xi s_\ell^\xi g \Lambda_{3j} \mathcal{R} - c_u^\xi \Lambda_{4j} g \mathcal{R} + c_u^\xi \Lambda_{4j} g),$$

$$B_{\ell j} \tilde{D} \xi = (-s_u^{\xi 2} c_\ell^\xi \Lambda_{3j} \mathcal{R} - s_u^{\xi 2} \Lambda_{4j} \mathcal{R} - c_u^\xi s_\ell^\xi \Lambda_{3j} s_u^\xi \mathcal{R} + c_u^{\xi 2} \Lambda_{4j}) \omega_+^4 - \xi (c_u^{\xi 2} \mathcal{R} \Lambda_{1j} - s_u^{\xi 2} \Lambda_{1j} \mathcal{R} - c_u^\xi \Lambda_{2j}) (c_u^\xi s_\ell^\xi + s_u^\xi c_\ell^\xi) \omega_+^2 - g s_u^\xi \xi^2 (-c_u^\xi s_\ell^\xi g \Lambda_{3j} \mathcal{R} - s_u^\xi c_\ell^\xi g \Lambda_{3j} \mathcal{R} + s_u^\xi g \Lambda_{4j} - s_u^\xi \Lambda_{4j} g \mathcal{R} + s_u^\xi c_\ell^\xi \Lambda_{2j} + c_u^\xi s_\ell^\xi \Lambda_{2j})$$

for $j = 1, 2$. In the above, the symbols c_u^ξ , c_ℓ^ξ , s_u^ξ and s_ℓ^ξ stand for $\cosh(\xi h_u)$, $\cosh(\xi h_\ell)$, $\sinh(\xi h_u)$ and $\sinh(\xi h_\ell)$ respectively and

$$\Lambda_j \equiv \Lambda_{j1} \cos(\omega_+ t) + \Lambda_{j2} \sin(\omega_+ t) = \int_{L_1}^{L_2} V_j(x, t) e^{i\xi x} dx$$

for $j = 1, \dots, 4$ with $V_1 = f_1^{(3)}$, $V_2 = f_3^{(3)}$, $V_3 = f_5^{(3)}$, and $V_4 = f_6^{(3)}$. The free-surface and interfacial wave elevations are then obtained from (2.3d) and (2.3g) with $m = 3$.

Appendix B. Multiple scale analysis

B.1. Perfect tuning Bragg resonance over a finite patch

For the steady solution, A and A^r are independent of t , and (4.2) and (4.3) become

$$\left(\frac{\partial^2}{\partial x^2} - \frac{\mathcal{M}\mathcal{N}}{C_g C_g^r} \right) \begin{Bmatrix} A \\ A^r \end{Bmatrix} = 0. \quad (\text{B } 1)$$

For the case in which the resonance-generated wave is a transmitted wave (i.e. $k^r = k_s$ or k_i), it can be shown that $\kappa^2 \equiv -\mathcal{M}\mathcal{N}/(C_g C_g^r) > 0$. In this case, the general solution to (B 1) takes the form

$$A(x) = C_1 \sin(\kappa x) + C_2 \cos(\kappa x), \quad A^r(x) = C_3 \sin(\kappa x) + C_4 \cos(\kappa x), \quad (\text{B } 2)$$

where C_j , $j = 1, \dots, 4$, are the unknown constants. If the resonant wave is a transmitted wave, the boundary conditions are $A^T(x) = A^r(x) = 0$ and $A(x) = a$ at $x = 0$, where a is the amplitude of the incident wave. From these boundary conditions, together with either (4.2) or (4.3), the four unknown constants C_j , $j = 1, \dots, 4$, can be solved. The final solution for A and A^T is

$$A(x) = a \cos(\kappa x), \quad A^T(x) = -\frac{\mathcal{N}}{\kappa C_g^r} a \sin(\kappa x). \quad (\text{B } 3)$$

From conservation of wave action, as in the one fluid case (cf. (3.1.17) in Mei *et al.* 2005), the following relation can be shown to obtain:

$$\left(\frac{\mathcal{N}}{\kappa C_g^r} \right)^2 = \frac{\mathcal{N} C_g}{\mathcal{M} C_g^r} = \frac{[\mathcal{R} + \lambda^2(1 - \mathcal{R})] C_g}{[\mathcal{R} + \lambda^2(1 - \mathcal{R})] C_g^r}. \quad (\text{B } 4)$$

Therefore, the solution for the amplitude of the resonance-generated wave in (B 3) can also be expressed as

$$|A^T(x)| = \left\{ \frac{[\mathcal{R} + \lambda^2(1 - \mathcal{R})] C_g}{[\mathcal{R} + \lambda^2(1 - \mathcal{R})] C_g^r} \right\}^{1/2} a |\sin(\kappa x)|. \quad (\text{B } 5)$$

Numerical evaluation of the dimensionless modulation wavenumber $\kappa^* = \kappa/(dkk^r)$ shows that κ^* increases as kh_u , kh_ℓ or \mathcal{R} decrease. This indicates that the modulation in $A^r(x)$ occurs more rapidly for stronger wave–bottom interactions. Also κ varies linearly with the bottom-topography amplitude.

For the case in which the resonance-generated wave is reflected (i.e. $k^r = -k_s$ or $-k_i$), it can be shown that $-\mathcal{M}\mathcal{N}/(C_g C_g^r) < 0$. Therefore by defining $\kappa^2 = \mathcal{M}\mathcal{N}/(C_g C_g^r)$ the general solution to (B 1) takes the form

$$A(x) = C_1 \sinh(\kappa x) + C_2 \cosh(\kappa x), \quad A^R(x) = C_3 \sinh(\kappa x) + C_4 \cosh(\kappa x). \quad (\text{B } 6)$$

The boundary conditions are $A^R(x)=0$ at $x=2L$ and $A(x)=a$ at $x=0$. Using these boundary conditions and either (4.2) or (4.3), we can solve for the four unknown coefficients and obtain finally for A and A^R :

$$A(x) = a \frac{\cosh \kappa(2L-x)}{\cosh 2\kappa L}, \quad (\text{B } 7)$$

$$A^R(x) = a \frac{\mathcal{N}}{\kappa C_g^r} \frac{\sinh \kappa(2L-x)}{\cosh 2\kappa L}. \quad (\text{B } 8)$$

B.2. Bragg resonance over a long patch of ripples

For a very long bottom patch of periodic ripples, the problem (away from the edges of the patch) can be cast in terms of the time evolution of a wave travelling over a periodic domain of bottom ripples. In this case, the governing equations are still (4.2) and (4.3) with the x dependencies dropped. If the resonant wave is a transmitted wave, sinusoidal modulation occurs in time. With the initial conditions $A(t)=a$ and $A^T(t)=0$ at $t=0$, we obtain that

$$A(t) = a \cos(\kappa^t t), \quad |A^T(t)| = a \left[\frac{\mathcal{R} + \lambda^2(1-\mathcal{R})}{\mathcal{R} + \lambda^r(1-\mathcal{R})} \right]^{1/2} |\sin(\kappa^t t)|, \quad (\text{B } 9)$$

where $\kappa^t = (-\mathcal{M}\mathcal{N})^{1/2}$.

It is now possible to relate $A^T(t)$ in (B 9) to $A^T(x)$ in (B 5) in terms of group velocity. In the special cases of same-mode resonance interactions or in the case of a homogeneous fluid (Liu & Yue 1998), the group velocity of the resonant wave, C_g^r , is the same as the group velocity of the incident wave, C_g , and $A^T(t)$ and $A^T(x)$ are related by the single group velocity $t = x/C_g$, as in the classical relationship between the spatial/temporal evolution of a single wave train (e.g. Gaster 1962). In the general case, $C_g \neq C_g^r$, and from (4.2) and (4.3), it can be readily shown that $A^T(x)$ in (B 5) is related to $A^T(t)$ in (B 9) by a factor of $(C_g/C_g^r)^{1/2}$ and the relation $t = x/(C_g C_g^r)^{1/2}$.

B.3. Detuned cases

For the detuned case, assume that the incident wave has a wavenumber of $k + \epsilon K$ and a frequency $\omega + \epsilon \Omega$, where $\mathcal{D}(k, \omega) = 0$ and $\Omega = C_g K$. On the rippled-bottom region ($0 \leq x \leq 2L$), let

$$(A, A^r) = a[F(x), F^r(x)]e^{-i\Omega t}. \quad (\text{B } 10)$$

Substitution of the above into (4.2) and (4.3) gives the differential equations for F and F^r :

$$\left[\frac{\partial^2}{\partial x^2} - i\Omega \left(\frac{1}{C_g} + \frac{1}{C_g^r} \right) \frac{\partial}{\partial x} - \frac{\Omega^2 + \mathcal{M}\mathcal{N}}{C_g C_g^r} \right] \begin{Bmatrix} F \\ F^r \end{Bmatrix} = 0. \quad (\text{B } 11)$$

The general solution to (B 11) can be written in the form

$$F(x) = C_1 e^{r_1 x} + C_2 e^{r_2 x}, \quad F^r(x) = C_3 e^{r_1 x} + C_4 e^{r_2 x}, \quad (\text{B } 12)$$

where r_1 and r_2 are the two roots of the characteristic equation. Based on the proper boundary conditions and the matching conditions (from substitution of (B 10) into

(4.2) or (4.3)), the unknown constants in (B 12) can be determined. In the following, for clarity, the results for the cases of resonant transmitted and reflected waves are described separately.

Case A

For the case in which the resonance-generated wave is transmitted over the rippled bottom, the discriminant of the characteristic equation of (B 11) is always negative, and r_1 and r_2 are

$$r_{1,2} = i\mathcal{B}[\Omega \pm (\Omega_0^2 + \Omega^2)^{\frac{1}{2}}], \tag{B 13}$$

where

$$\mathcal{B} \equiv \frac{1}{2} \left(\frac{1}{C_g^r} - \frac{1}{C_g} \right) \quad \text{and} \quad \Omega_0 \equiv 2 \frac{|\mathcal{M}\mathcal{N}C_gC_g^r|^{\frac{1}{2}}}{|C_g - C_g^r|}.$$

In the incident side ($x < 0$), we have $A(x) = a \exp [i(Kx - \Omega t)]$ and $A^T(x) = 0$, which lead to the boundary conditions $F(x) = 1$ and $F^T(x) = 0$ at $x = 0$. From these boundary conditions, we obtain

$$F(x) = e^{i\mathcal{B}\Omega x} \left[-i\frac{\Omega}{2\kappa} \left(\frac{1}{C_g^r} + \frac{1}{C_g} \right) \sin(\kappa x) + \cos(\kappa x) \right], \tag{B 14a}$$

$$F^T(x) = -e^{i\mathcal{B}\Omega x} \frac{\mathcal{N}}{\kappa C_g^r} \sin(\kappa x), \tag{B 14b}$$

where $\kappa = \mathcal{B}(\Omega_0^2 + \Omega^2)^{1/2}$. On the transmission side ($x > 2L$), we have

$$A(x) = aA^c e^{i(Kx - \Omega t)}, \quad A^T(x) = aT e^{i(K^r x - \Omega t)}, \tag{B 15}$$

where A^c and T are the transmission coefficients of the incident and resonance-generated waves and are given by

$$A^c = e^{2i\mathcal{B}\Omega L} \left[-i\frac{\Omega}{2\kappa} \left(\frac{1}{C_g^r} + \frac{1}{C_g} \right) \sin(2\kappa L) + \cos(2\kappa L) \right], \quad T = -e^{2i\mathcal{B}\Omega L} \frac{\mathcal{N}}{\kappa C_g^r} \sin(2\kappa L). \tag{B 16}$$

For a surface mode incident wave, as an example, because the characteristic equation has no critical value, for all frequencies only modulation occurs. The amplitude of modulation is independent of the length of the rippled patch but increases as the frequency detuning decreases. Frequency of modulation varies with the frequency detuning because the length has been normalized with $\kappa_0 = \kappa|_{\Omega=0} = \mathcal{B}\Omega_0$.

Case B

For the case in which the resonance-generated wave is reflected, we have

$$r_{1,2} = [i\Omega \pm (\Omega_0^2 - \Omega^2)^{\frac{1}{2}}]. \tag{B 17}$$

Clearly, Ω_0 is the cutoff frequency. For $|\Omega| < \Omega_0$, $F(x)$ ($F^R(x)$) has both sinusoidally varying and exponentially decaying (growing) parts in x . For $|\Omega| > \Omega_0$, $F(x)$ and $F^R(x)$ are purely sinusoidal in x . For critical detuning $\Omega = \Omega_0$, $F(x)$ ($F^R(x)$) has a sinusoidal variation in x with the amplitude linearly decaying (growing) with x .

In this case, the boundary conditions are $F(x) = 1$ at $x = 0$ and $F^R(x) = 0$ at $x = 2L$. Based on these boundary conditions, we can obtain $F(x)$ and $F^R(x)$. Specifically, for

$|\Omega| < \Omega_0$, we have

$$F(x) = \frac{e^{i\mathcal{B}\Omega x}}{\gamma^+ - \lambda^+ e^{4\kappa L}} [\gamma^+ e^{\kappa x} - \lambda^+ e^{\kappa(4L-x)}], \quad F^R(x) = \frac{e^{i\mathcal{B}\Omega x}}{\gamma^+ - \lambda^+ e^{4\kappa L}} [e^{\kappa x} - e^{\kappa(4L-x)}], \quad (\text{B } 18)$$

where $\kappa = \mathcal{B}(\Omega_0^2 - \Omega^2)^{1/2}$, $\gamma^+ = (i\Omega - r_1 C_g^r)/\mathcal{N}$ and $\lambda^+ = (i\Omega - r_2 C_g^r)/\mathcal{N}$. Thus we have on the incident side ($x < 0$)

$$A(x) = a e^{i(Kx - \Omega t)}, \quad A^R(x) = a R e^{i(K^R x - \Omega t)} \quad (\text{B } 19)$$

and on the transmission side ($x > 2L$)

$$A(x) = a A^c e^{i(Kx - \Omega t)}, \quad A^R(x) = 0, \quad (\text{B } 20)$$

where the reflection coefficient of the resonance-generated wave, R , and the transmission coefficient of the incident wave, A^c , are

$$R = \frac{1}{\gamma^+ - \lambda^+ e^{4\kappa L}} [1 - e^{4\kappa L}], \quad A^c = \frac{e^{2i\mathcal{B}\Omega L}}{\gamma^+ - \lambda^+ e^{4\kappa L}} (\gamma^+ - \lambda^+) e^{2\kappa L}. \quad (\text{B } 21)$$

If $|\Omega| > \Omega_0$, the solution is obtained from the above (for $|\Omega| < \Omega_0$) by replacing κ by $i\kappa$.

At the critical frequency $|\Omega| = \Omega_0$, $r_1 = r_2$. The general solution in (B 12) must be changed to the form $F(x) = (C_1 + C_2 x) \exp(r_1 x)$ and $F^R(x) = (C_3 + C_4 x) \exp(r_2 x)$. Using the same boundary condition, $F(x) = 1$ at $x = 0$ and $F^R(x) = 0$ at $x = 2L$, we obtain

$$F(x) = \left[1 + \frac{i\Omega (C_g^r \mathcal{B} - 1)}{\hat{\mathcal{B}}} x \right] e^{i\mathcal{B}\Omega x}, \quad F^R(x) = \frac{\mathcal{N}(2L - x)}{\hat{\mathcal{B}}} e^{i\mathcal{B}\Omega x}, \quad (\text{B } 22)$$

where $\hat{\mathcal{B}} = C_g^r + i\Omega(L - \mathcal{B}C_g^r)$. In this case, R and A^c are

$$R = \frac{2\mathcal{N}L}{C_g^r + i\Omega L(1 - C_g^r \mathcal{B})}, \quad A^c = \left[1 + \frac{2i\Omega L(C_g^r \mathcal{B} - 1)}{C_g^r + i\Omega L(1 - C_g^r \mathcal{B})} \right] e^{2i\mathcal{B}\Omega L}. \quad (\text{B } 23)$$

REFERENCES

- ALAM, M.-R. 2008 Interaction of waves in a two-layer density stratified fluid. PhD thesis, Massachusetts Institute of Technology, Cambridge, MA, USA.
- ALAM, M.-R., LIU, Y. & YUE, D. K. P. 2009 Bragg resonance of waves in a two-layer fluid propagating over bottom ripples. Part II. Numerical simulation. *J. Fluid Mech.* **624**, 225–253.
- ALAM, M.-R. & MEI, C. C. 2007 Attenuation of long interfacial waves over a randomly rough seabed. *J. Fluid Mech.* **587**, 73–96.
- ANTENUCCI, J. P. & IMBERGER, J. 2001 On internal waves near the high-frequency limit in an enclosed basin. *J. Geophys. Res.* **106** (C 10), 22465–22474.
- ARDHUIN, F. & HERBERS, T. H. C. 2002 Bragg scattering of random surface gravity waves by irregular seabed topography. *J. Fluid Mech.* **451**, 1–33.
- ARDHUIN, F. & MAGNE, R. 2007 Scattering of surface gravity waves by bottom topography with a current. *J. Fluid Mech.* **576**, 235–264.
- BAINES, P. G. 1995 *Topographic Effects in Stratified Flows*. Cambridge University Press.
- BAINES, P. G. 1997 *Topographic Effects in Stratified Flows*. In *Cambridge Monographs on Mechanics* (ed. G. K. Batchelor & L. B. Freund). Cambridge University Press.
- BALL, F. 1964 Energy transfer between external and internal gravity waves. *J. Fluid Mech.* **19**, 465–478.

- BELZONS, M., GUAZZELLI, E. & PARODI, O. 1988 Gravity-waves on a rough bottom – experimental-evidence of one-dimensional localization. *J. Fluid Mech.* **186**, 539–558.
- BOEGMAN, L., IMBERGER, J., IVEY, G. N. & ANTENUCCI, J. P. 2003 High-frequency internal waves in large stratified lakes. *Limnol. Oceanogr.* **48** (2), 895–919.
- CHEN, Y. & LIU, P. L.-F. 1996 On interfacial waves over random topography. *Wave Mot.* **24** (2), 169–184.
- CUMMINS, P. F., VAGLE, S., ARMI, L. & FARMER, D. M. 2003 Stratified flow over topography: upstream influence and generation of nonlinear internal waves. *Proc. R. Soc. Lond. A* **459** (2034), 1467–1487.
- DAVIES, A. G. 1982 The reflection of wave energy by undulation on the seabed. *Dyn. Atmos. Oceans* **6**, 207–232.
- DIAS, F. & VANDEN-BROECK, J.-M. 2003 On internal fronts. *J. Fluid Mech.* **479**, 145–154.
- FARMER, D & ARMI, L 1999 The generation and trapping of solitary waves over topography. *Science* **283** (5399), 188–190.
- GARGETT, A. E. & HUGHES, B. A. 1972 On the interaction of surface and internal waves. *J. Fluid Mech.* **52** (01), 179–191.
- GARRETT, C. & MUNK, W. 1975 Space-time scales of internal waves: A progress report. *J. Geophys. Res.* **80** (C3), 291–298.
- GARRETT, C. & MUNK, W. 1979 Internal waves in the ocean. *Annu. Rev. Fluid Mech.* **11** (1), 339–369.
- GASTER, M. 1962 A note on the relation between temporally-increasing and spatially-increasing disturbances in hydrodynamic stability. *J. Fluid Mech.* **14**, 222–224.
- GUAZZELLI, E., REY, V. & BELZONS, M. 1992 Higher-order bragg reflection of gravity surface waves by periodic beds. *J. Fluid Mech.* **245**, 301–317.
- HASSELMANN, K. 1966 Feynman diagrams and interaction rules of wave-wave scattering processes. **4** (1), 1–32.
- HEATHERSHAW, A. D. & DAVIES, A. G. 1985 Resonant wave reflection by transverse bedforms and its relation to beaches and offshore bars. *Mar. Geol.* **62**, 321–338.
- HILL, D. F. 2004 Weakly nonlinear cubic interaction between surface waves and interfacial waves: an analytic solution. *Phys. Fluids* **16** (3), 839–842.
- HILL, D. F. & FODA, M. A. 1996 Subharmonic resonance of short internal standing waves by progressive surface waves. *J. Fluid Mech.* **321**, 217–233.
- HILL, D. F. & FODA, M. A. 1998 Subharmonic resonance of oblique interfacial waves by a progressive surface wave. *Proc. R. Soc. Lond. A* **454** (1972), 1129–1144.
- HOLT, J. T. & THORPE, S. A. 1997 The propagation of high frequency internal waves in the Celtic Sea. *Deep-Sea Res. Pt I* **44** (12), 2087–2116.
- JAMALI, M. 1998 Surface wave interaction with with oblique internal waves. PhD thesis, University of British Columbia, Vancouver, Canada.
- JAMALI, M., LAWRENCE, G. A. & SEYMOUR, B. 2003 A note on the resonant interaction between a surface wave and two interfacial waves. *J. Fluid Mech.* **491**, 1–9.
- KIRBY, J. T. 1986 A general wave equation for waves over rippled beds. *J. Fluid Mech.* **162**, 171–186.
- KUDRYAVTSEV, V. N. 1994 The coupling of wind and internal waves: modulation and friction mechanisms. *J. Fluid Mech.* **278**, 33–62.
- LAMB, H. 1932 *Hydrodynamics*. Dover.
- LIU, Y. & YUE, D. K. P. 1998 On generalized Bragg scattering of surface waves by bottom ripples. *J. Fluid Mech.* **356**, 297–326.
- McKEE, W. D. 1996 Bragg resonances in two-layer fluid. *J. Austral. Math. Soc. B* **37** (3), 334–345.
- MEI, C. C. 1985 Resonant reflection of surface water waves by periodic sandbars. *J. Fluid Mech.* **152**, 315–335.
- MEI, C. C., STIASSNIE, MICHAEL & YUE, DICK K.-P. 2005 *Theory and Applications of Ocean Surface Waves. Part 1.2. Advanced Series on Ocean Engineering*, vol. 23. World Scientific.
- MELVILLE, W. K. & HELFRICH, KARL R. 1987 Transcritical two-layer flow over topography. *J. Fluid Mech.* **178**, 31–52.
- MIROPOL'SKY, Y. Z. 2001 *Dynamics of Internal Gravity Waves in the Ocean: Atmospheric and Oceanographic Sciences Library* (trans. and ed. O. D. Shishkina), vol. 24. Kluwer Academic Publishers.

- OLBERS, D. J. & HERTERICH, K. 1979 The spectral energy transfer from surface waves to internal waves. *J. Fluid Mech.* **92** (2), 349–379.
- THORPE, S. A. 1975 The excitation, dissipation, and interaction of internal waves in the deep ocean. *J. Geophys. Res.* **80** (3), 328–337.
- THORPE, S. A., KEEN, J. M., JIANG, R. & LEMMIN, U. 1996 High-frequency internal waves in lake Geneva. *Phil. Trans.* **354** (1705), 237–257.
- VELETOS, A. S. & SHIVAKUMAR, P. 1993 Sloshing response of layered liquids in rigid tanks. *Tech Rep.* BNL-52378, Brookhaven National Lab., Upton, NY, USA.
- WEN, F. 1995 Resonant generation of internal waves on the soft sea bed by a surface water wave. *Phys. Fluids* **7** (8), 1915–1922.